ESTIMATION OF STATOR RESISTANCE IN SENSOR-LESS INDUCTION MOTOR DRIVE USING MRAS

DISSERTATION

SUBMITTED IN PARTIAL FULFILLMENT OF THE RQUIREMENTS
FOR THE AWARD OF THE DEGREE
OF

MASTER OF TECHNOLOGY
IN
CONTROL AND INSTRUMENTATION

Submitted by:

AVINASH
2K14/C&I/20

Under the supervision of

Dr. Mini Sreejeth

DEPARTMENT OF ELECTRICAL ENGINEERING
DELHI TECHNOLOGICAL UNIVERSITY
(Formerly Delhi College of Engineering)
Bawana Road, Delhi-110042

2016

DEPARTMENT OF ELECTRICAL ENGINEERING

DELHI TECHNOLOGICAL UNIVERSITY
(Formerly Delhi College of Engineering)
Bawana Road, Delhi-110042

CERTIFICATE

I, **Avinash**, Roll No. 2K14/C&I/20 student of **M. Tech. (Control and Instrumentation)**, hereby declare that the dissertation titled **"Estimation of Stator Resistance in Sensor-less Induction Motor Drive Using MRAS "** under the supervision of Dr. Mini Sreejeth, Assistant Professor, Department of Electrical Engineering, Delhi Technological University in partial fulfillment of the requirement for the award of the degree of Master of Technology has not been submitted elsewhere for the award of any Degree.

Place: Delhi **AVINASH**

Date: 30.06.2016

Dr. MINI SREEJETH
Assistant Professor
Department of Electrical Engineering
Delhi Technological University

ACKNOWLEDGEMENT

I would like to express my sincere gratitude to Dr. Mini Sreejeth for her guidance and assistance in the thesis. The technical discussions with her were always been very insightful, and I will always be indebted to her for all the knowledge she shared with me. She always helped me in all the technical and non-technical issues during the production of this thesis. Without her consistent support, encouragement and valuable inputs, this project would not have become possible.

I would like to express my deep gratitude to Prof. Madhusudan Singh, Head, Department of Electrical Engineering for providing his support during my project.

An assemblage of this nature could never have been attempted without reference to and inspiration from the works of others whose details are mentioned in reference section. I acknowledge my indebtedness to all of them.

I am thankful to all my classmates and the department research scholars for their co-operation and unfailing help during the project work.

I am grateful to all my friends who made my stay in Delhi, an unforgettable and rewarding experience.

Finally, I feel great reverence for all my family members and the Almighty, for their blessings and for being a constant source of encouragement.

AVINASH

(2K14/C&I/20) M.Tech
(Control and Instrumentation)
Delhi Technological University

ABSTRACT

Industrial motor drive applications are usually complex and expensive. Most industries invest time and effort to implement drives which are low-cost, reliable, energy efficient and require low maintenance. In this field, the Induction motor (IM) is popular for its superior performance compared to its counterparts. There are two types of IM- squirrel cage IM and wound rotor IM both widely used. The popularity of the squirrel cage induction machine is attributed to its ruggedness (high output power to size ratio) and simplicity of construction. Recent advances in power electronics such as the Voltage Source Inverter (VSI) based drives have enabled variable speed control of IM's. VSI based drive converts DC voltage into three phase voltage of variable magnitude and frequency based on requirements for motor control. This thesis has its foundation on a certain form of control called Indirect Vector control based on frame transformations, estimators and error based controllers.

This thesis work presents a new sensor less vector control scheme consisting on the one hand of a speed estimation algorithm which overcomes the necessity of the speed sensor and on the other hand of a stator resistance estimation algorithm.

In this work, the design includes stator resistance estimation and rotor speed estimation from measured stator terminal voltages and currents. The estimated stator resistance is given to the speed estimation block. The rotor speed is used as feedback in an indirect vector control system achieving the speed control without the use of shaft mounted transducers. The scheme is simulated using a 1.5HP, 460V, 50Hz induction motor.

CONTENTS

LIST OF TABLES

LIST OF FIGURES

LEGENDS

$d^e - q^e$	Synchronously rotating reference frame (or rotating frame) direct and quadrature axes
$d^s - q^s$	Stationary reference frame direct and quadrature axes.
f	Frequency (Hz)
I_d	Dc current (Ampere)
I_L	Rms load current
I_m	Rms magnetizing current
I_f	Machine field current
i_{dr}^s	d^s - axis rotor current
i_{ds}^s	d^s- axis stator current
i_{qr}^s	q^s - axis rotor current.
i_{qs}^s	q^s - axis stator current
i_{qr}	q^e- axis rotor current
i_{dr}	d^e - axis rotor current
i_{ds}	d^e - axis stator current
i_{qs}	q^e - axis stator current
i_{abc}^*	Command current
i_{abc}	Actual current
J	Moment of inertia (Kg-m^2)
X_r	Rotor Reactance (Ohm)
X_s	Synchronous reactance
X_{ds}	d^e- axis synchronous reactance
X_{lr}	Rotor leakage reactance
X_{ls}	Stator leakage reactance
X_{qs}	q^e- axis synchronous reactance
K	Constant gain

K_T	Torque constant
θ_e	Angle of Synchronously rotating frame
θ_r	Rotor angle
θ_{sl}	Slip angle
L_m	Magnetizing inductance
L_r	Rotor inductance
L_s	Stator inductance
L_{lr}	Rotor leakage inductance
L_{ls}	Stator leakage inductance
p	Differential operator
P	Number of poles
R_r	Rotor resistance
R_s	Stator resistance
T_e	Developed torque
T_{em}	Electromagnetic torque
T_r	Rotor time constant
v_{dr}^s	d^s -axis rotor voltage
v_{qr}^s	q^s - axis rotor voltage
v_{ds}^s	d^s - axis stator voltage
v_{qs}^s	q^s - axis stator voltage
v_{qr}	q^e - axis rotor voltage
v_{dr}	q^e- axis rotor voltage
v_{qs}	q^e - axis stator voltage
v_{ds}	d^e - axis stator voltage
Ψ_a	Armature reaction flux linkage
Ψ_f	Field flux linkage
Ψ	Airgap flux linkage
Ψ_r	Rotor flux linkage
Ψ_{dr}^s	d^s - axis rotor flux linkage
Ψ_{qr}^s	q^s - axis rotor flux linkage
Ψ_{ds}^s	d^s- axis stator flux linkage
Ψ_{qs}^s	q^s - axis stator flux linkage

Ψ_{qr}	q^e - axis rotor flux linkage
Ψ_{dr}	d^e - axis rotor flux linkage
Ψ_{qs}	q^e - axis stator flux linkage
Ψ_{ds}	d^e - axis stator flux linkage
ω_e	Stator frequency
ω_m	Rotor mechanical speed
ω_r	Rotor electrical speed
ω_{sl}	Slip frequency
σ	Motor leakage coefficient

Superscript

*	Command signal
~	Estimated quantity
r	Rotor reference frame
s	Stator reference frame

ABBREVIATION AND ACRONYMS

AC	Alternating Current
EMF	Electromotive Force
DC	Direct Current
DSP	Digital Signal Processing
EKF	Extended Kalman Filter
ELO	Extended Luenberger Observer
FOP	Field Oriented Principle
EMF	Electro-motive Force
FL	Fuzzy Logic
FLC	Fuzzy Logic Control
GA	Genetic Algorithm
HPF	High Pass Filter
LPF	Low-Pass Filters
NN	Neural Network
MMF	Magneto-motive Force
IGBT	Insulated Gate Bipolar Transistor
IM	Induction Motor
MRAC	Model Reference Adaptive Control
MRAS	Model Reference Adaptive System
.	
PWM	Pulse Width Modulation
SVPWM	Space Vector Pulse Width Modulation
SMC	Sliding Mode Control

CHAPTER 1
INTRODUCTION

1.1 INTRODUCTION

Over the past decades DC machines were used extensively for variable speed applications due to the decoupled control of torque and flux that can be achieved by armature and field current control respectively. DC drives are advantageous in many aspects as in delivering high starting torque, ease of control and nonlinear performance. But due to the major drawbacks of DC machine such as presence of mechanical commutator and brush assembly, DC machine drives have become obsolete today in industrial applications.

The robustness, low cost, the better performance and the ease of maintenance make the asynchronous motor advantageous in many industrial applications or general applications. Squirrel cage induction motors (SCIM) are more widely used than all the rest of the electric motors as they have all the advantages of AC motors and are cheaper in cost as compared to Slip Ring Induction motors; require less maintenance and rugged construction [1]. Because of the absence of slip rings, brushes maintenance duration and cost associated with the wear and tear of brushes are minimized. Due to these advantages, the induction motors have been the execution element of most of the electrical drive system for all related aspects: starting, braking, speed change and speed reversal etc.

1.2 INDUCTION MOTOR DRIVES

Power semiconductor devices constitute the heart of modern power electronics equipment's. They are used in converters in the form of a matrix of on off switches, and are helping in conversion of power from ac to dc, dc to dc and ac to ac at the same or at different frequencies. The switching mode power conversion gives high efficiency , the disadvantage is due to the nonlinearity of the switches, harmonics are generated at both the supply and load sides .Converters are widely used in many application such as heating , lighting controls , ac and dc power supplies , electrochemical processes , ac and dc motor drives , active harmonic filtering and static var generation etc. Due to the use of power semiconductor devices in power electronic equipment may hardly increase 25 -35 percent cost. The total cost of equipment and performance may highly influence by the characteristics of the devices. An engineer designs the equipments according to the characteristics of the devices so that reliable, and cost effective system with optimum performances can be achieved. The advancement of microelectronics greatly contribute the knowledge of power device material, processing, fabrication, modeling and simulation [1]. In recent years, dc motor was used mostly in areas where we require variable operation was required, since there flux and torque could be easily controlled by the field and armature current. The separately excited dc motor has been used in many applications, where there was a requirement of fast response and four quadrant operation with near zero and high speed. However the dc motor have some disadvantage , which are mainly due to the existence of the commutator and the brushes and because of this they require regular maintenance, therefore they cannot be used in corrosive or explosives environment and they have limited commutator capability under high speed, high voltage conditions. These problems can be overcome by using alternating current motors, which can be rugged and simple in structure.

Variable speed ac drives have been used in past to perform relatively undemanding roles in application which preclude the use of dc motor, because of the commutator limits and working environment. The progress in the field of power electronics, the trend is towards cheaper and more effective power converters, and a single phase motor ac drives completely favorably on a purely economic basis with a dc drives.

The various ac drive systems, which contain the squirrel cage induction motor is simple and rugged and is one of the cheapest machines which is available in all power ratings. With the rapid developments in the field of microelectronics, torque control of various types of ac machines will become a commonly used technique, even though high dynamic performance is not required. It is possible to contribute the energy saving by the application of intelligent control of the torque and flux producing components of stator currents.

Adjustable speed AC drives have the preferred choice in many industrial application where control speed is required. The availability of fast and efficient solid state power semiconductor switches (IGBTs) has resulted in voltage sources, PWM controlled inverters become a standard configurations in the power range to 500kW.

The control and estimation of ac drives in general are more complex than those of dc drives, and this complexity increases if high performances are demanded. The main reasons for complexity are the need of variable frequency converter power supplies, the complex dynamics of ac machines, machine parameter variation.

The vector control theory has been receiving much attention because of better steady and dynamic performance over conventional control methods in controlling motors torque and speed. The vector control technique has been widely used in several electric drive applications. By providing decoupling of flux and torque control commands, the vector control navigate an AC motor drive similar to separately excited DC motor drive without sacrificing the quality of the dynamic performance. Within this scheme, a rotational transducer like a tachogenerator, an encoder or a resolver, is mounted to establish the speed feedback. However, this speed sensor may lower the system reliability, increase device investment and complicate the implementation. Therefore, a speed sensor less drive has been used in modern industrial application. In various vector control schemes, the speed sensorless vector control has been a relevant area of interest for many researchers due to its low drive cost, easy maintenance and high reliability. There are two parameters which are required in speed sensorless vector control of induction motor, the motor flux and speed estimation. These parameters are required for establishing the outer speed loop feedback and also in the flux and torque control algorithms. . In order to get better performance of sensorless vector control, different methods of speed estimation have been proposed. Such as, model reference adaptive system (MRAS), direct calculation method, luenberger Observers, extended Kalman filter (EKF) and Estimators using artificial intelligence etc [1]. Out of all the speed estimation methods, MRAS-based speed sensorless estimation has been commonly used in AC speed regulation systems due to its good performance and ease of implementation. In order to design MRAS for sensorless speed estimation, first we have to model the induction motor dynamic model. In induction motor, inputs to the motor are stator currents and voltages and output is rotor speed. That’s why, while choosing reference model for MRAS, we have to form a rotor flux equation in the form of stator side parameters.

With advancements in the power electronics and intelligent control techniques, the torque and speed control of an induction motor are easily realizable, which was earlier thought to be very difficult and complex. There are different methods for controlling the speed of an induction motor, some are open loop and closed loop v/f control techniques, Vector or Field Oriented Control , Direct Torque Control (DTC) and Sensor-Less Control, these control methods are used for speed control of IM. Brief explanation of all these methods is given in the following sections.

1.3 SCALAR CONTROL

Scalar control, as the name implies, deals only with magnitude variation of the control variables like frequency and voltage. For example, the flux is controlled by the variation of voltage of a machine, whereas torque control is achieved through variation in slip or frequency [1]. However torque and flux being a functions of voltage and frequency respectively, there is an inherent coupling effect in the torque and flux producing components. Due to that scalar controlled has slow transient response and therefore not suitable for high performance applications. As compared to the scalar control technique, in vector control or field oriented control, both magnitude and the phase is controlled, Scalar controlled drives give somewhat inferior performances, but they are easy implemented. Scalar controlled drives have been widely used in the industry. But their importance has to be diminished day by day, because of the superior performance of vector controlled drives.

1.4 VECTOR OR FIELD-ORIENTED CONTROL

Scalar control is easy to implement, but due to inherent coupling effect of both flux and the torque producing components it gives sluggish response. As a result, system became unstable because of high order system harmonics. Let us consider a example, if the torque is increased by increasing the slip, the flux tends to decrease. This flux variation then compensated by sluggish flux control loop feeding additional voltage. This temporary dipping of the flux reduces the torque sensitivity with slip and increase the response time of the system. These problems can be solved by vector control or field oriented control. The invention of the vector control in 1970s, and induction motor can be controlled like a separately excited dc motor, Because of the performance similar to a dc machine, vector control is known as orthogonal, decoupling, or trans vector control. Vector control is applicable to both the synchronous motor drives and induction motor drives. Vector control method, particularly for the modern sensor-less vector control is very complex and the use of

DSP is mandatory. Depending on the method of determination of the flux angle, vector control is divided into direct and indirect vector controls.

1.4.1 Dc Drive Analogy

Ideally, the operation of a vector controlled induction motor drive is similar to a separately excited dc motor drive in Fig 2.1. After neglecting the armature reaction effect and field saturation effect in case of dc machine, the developed torque is given by

$$T_e = K_t \Psi_f \Psi_a = K_t' I_f I_a \tag{1.1}$$

Where, I_a = armature current
And I_f = field current

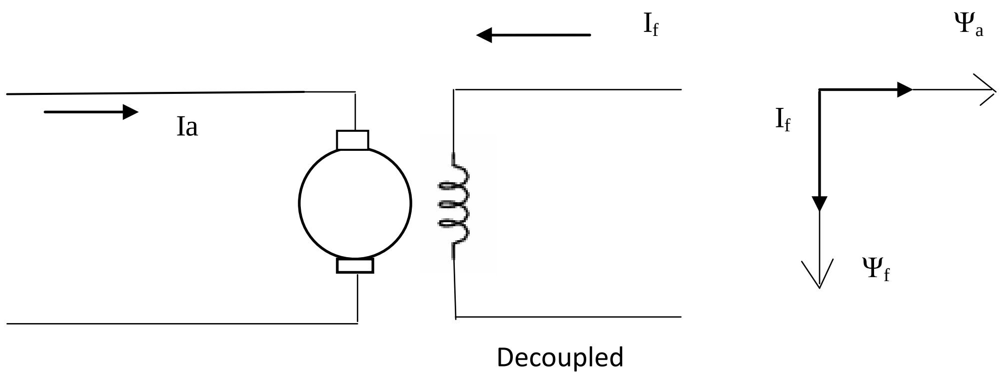

Fig 1.1 Separately excited dc motor

DC machine is constructed in such a way that the field flux $\hat{\Psi}_f$, which is produced by the field current I_f *is* perpendicular to the armature flux Ψ_a, which is produced by the armature current I_a. These space vectors are orthogonal and decoupled in nature and stationary in space. This means that, when the torque is controlled by the armature currentI_a, the field flux $\Psi_f$is not affected and we get the fast transient response and high torque ampere ratio [1]. Similarly in the same manner, because of decoupling, when the field current I_f is controlled, it affects only the field flux Ψ_f, but there are no effects on the armature flux Ψ_f flux. The induction motor due to inherent coupling problems cannot give such a fast response. The performance of an induction motor can be extended, if the machine is considered in a synchronously rotating reference frame ($d^e - q^e$). In synchronously rotating reference frame, the sinusoidal variables appear as a dc quantity in steady. The Figure 1.2 shows that an induction motor with a inverter and a vector control in front end, which receives a signal i_{ds}^* and i_{qs}^*. In a synchronously rotating reference frame these currents i_{ds}^* and i_{qs}^* are the direct axis component and the quadrature axis component of the stator current, respectively.

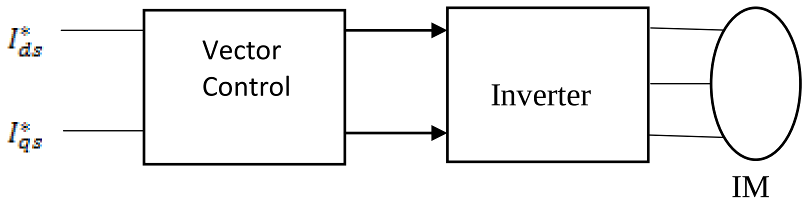

Fig 1.2 Vector controlled induction motor

In vector control the direct axis current i_{ds} is analogous to field current I_f and the quadrature axis current i_{qs} is analogous to armature current I_a of dc machine. Therefore, the torque in terms of i_{ds} *and* i_{qs} is given as,

$$T_e = K_t \hat{\Psi}_r \, i_{qs} = K_t \, i_{qs} \, i_{ds} \tag{1.2}$$

Where $\hat{\Psi}_r$ = absolute peak value of sinusoidal space vector.

This performance of an induction motor similar to a dc machines is only possible if i_{ds} is in the direction of $\hat{\Psi}_r$ and i_{qs} is perpendicular to it, which results that when i_{qs}^* is controlled, it affects the i_{qs} current only, but not affect the flux $\hat{\Psi}_r$.

Similarly in the same way, when i_{ds}^* is controlled, it controls the flux only and not the i_{qs} component of current. In all operating condition this orientation of current is essential in a vector control drive.

1.4.2 Principle of Vector Control

The implementation of vector control is discussed in the Fig 1.3. In the Figure the machine model is in synchronously rotating reference frame. Assumed a unity current gain of the inverter which is not shown in the Figure 1.3. The internal conversions of a machine model are shown on the right. The machine terminal phase currents i_a , i_b *and* i_c are converted into i^s_{ds} and i^s_{qs} components by 3ϕ to 2ϕ transformation.

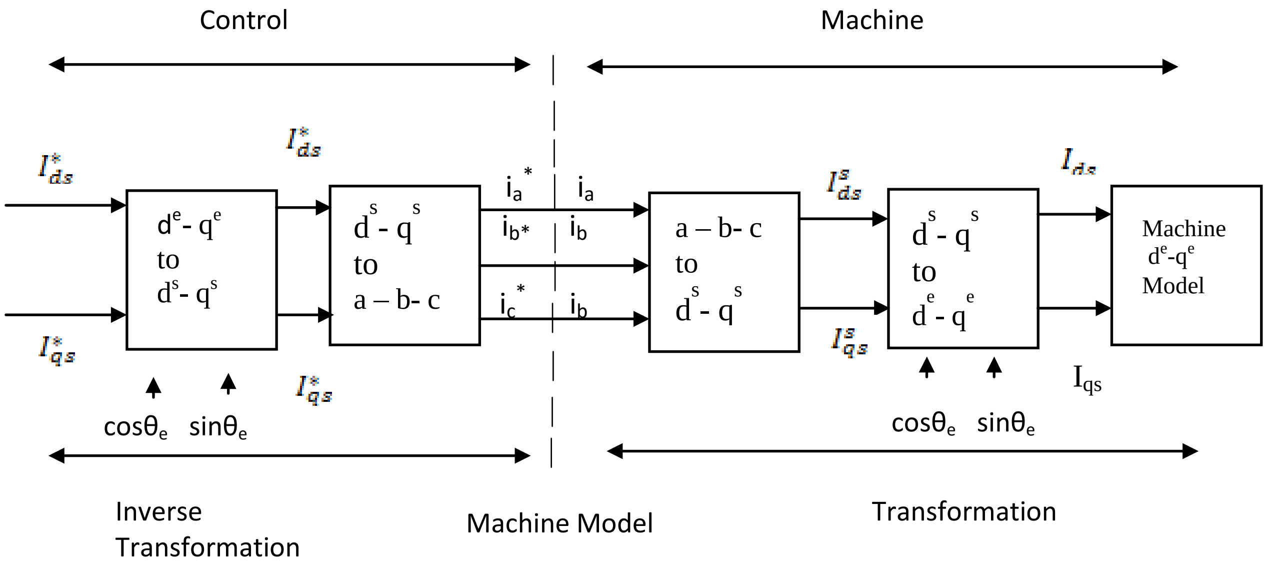

Fig 1.3 Vector control implementation principle with machine ($d^e - q^e$) model

Then we convert these into a synchronously rotating frame with the help of unit vector components $\cos\theta_e$ and $\sin\theta_e$, before applying them to $d^e - q^e$machine model, as shown in Fig 1.3. The inverse transformation of two stage made by controller as shown, so that the control currents i^*_{ds} and i^*_{qs} corresponds to machine currents i_{ds} and i_{qs} , respectively [1]. The response to $i_{ds}$and i_{qs} is instantaneous because the inverse transformation and transformation including the inverter do not incorporate any dynamics.

1.4.3 Dynamic d-q Model

The stator of an induction motor consists of a three phase balanced distributed windings with each phase separated by other two windings by 120 degrees in space [1]. When the current flows through these windings, a three phase rotating magnetic field is produced. The dynamic behavior of an induction machine is taken into account, in an adjustable speed drive system, using a power electronics converter. The study of a dynamic performance of the machine is complex due to the coupling effect of the stator and rotor windings, also the coupling coefficient varies with a rotor position. So, a set of differential equations with the time varying coefficients is describing the machine model [1]. To derive the dynamic model of the machine, we have to take some assumptions:

- No saliency effects i.e. machine inductance is independent of the rotor position.
- Stator windings are arranged , so as to produce sinusoidal mmf distributions.
- The effects of stator slots may be neglected.
- There is no fringing of the magnetic circuit.
- There is negligible eddy current and the hysteresis effects.

A three phase balanced supply is given to the induction motor from the power converter. For dynamic modeling of the motor, two axes theory is used [1]. According to this theory, the time varying parameters can be expressed in the mutually perpendicular direct (*d*) and the quadrature (*q*) axis. For the representation of the *d-q* dynamic model of machine a stationary or rotating reference frame is assumed.

In steady state conditions, only the per-phase equivalent circuit of the machine is valid. Whereas the high performance drive control, such as vector control or field oriented control is based on the dynamic d-q model of the machine. It is similar to the transformer with moving secondary, where as the coupling coefficients between the stator and rotor phases changes with change of rotor position θ_r . The model of the machine tends to be very complex, which is described by the differential equations, with time varying mutual inductances. A three phase machine is represented by an equivalent two phase's machine, where $d^s - q^s$) corresponding to the stator direct and quadrature axes, and$(d^r - q^r)$ *correspond* to the rotor direct and quadrature axes. Although it is simple, but the problem related to time varying parameters remain there.

In 1920 a new theory of electric machine, proposed by R. H Park and his analysis is to solve this problem. He formulated a change of variables, which associated with stator windings of synchronous machine like the voltage, current and flux linkage with variables associated with fictitious windings rotating with the rotor at a synchronous speed. He referred, the stator variables to a synchronously rotating reference frame fixed in the rotor. With such transformations called the Park's transformation, showed that all the time varying inductances was eliminated that occur due to an electric circuit in relative motion and electric circuit with varying magnetic reluctance is eliminated.

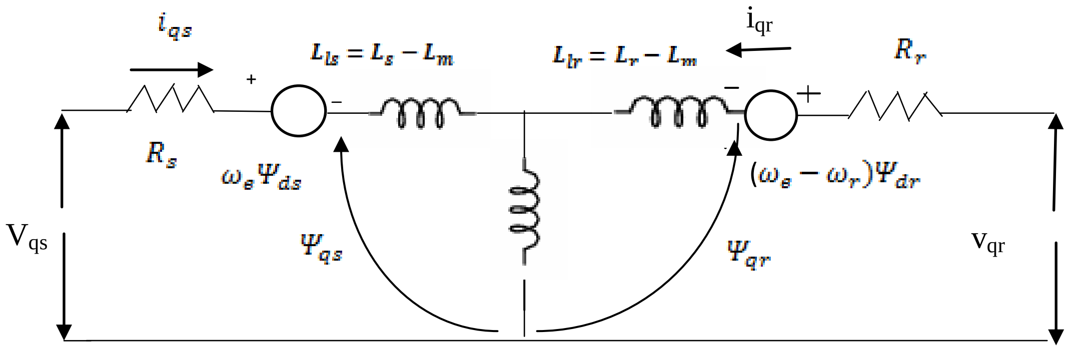

Fig 1.4 Dynamic $d^e - q^e$) equivalent circuit of machine $(q^e$ - axis)

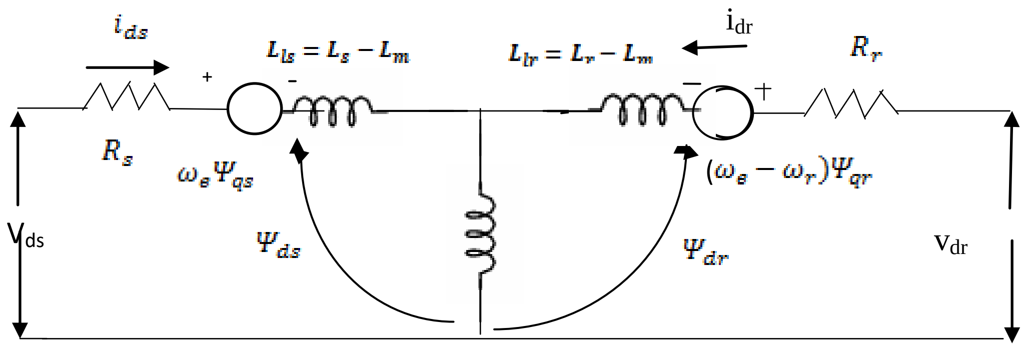

Fig 1.5 Dynamic $d^e - q^e$) equivalent circuit of machine (d^e - axis)

The above Figure shows the $d^e - q^e$ dynamic model equivalent circuit. A special advantage of $d^e - q^e$ dynamic model of the machine is that all the sinusoidal variables in stationary frame appear as a dc quantity in synchronous frame. From above model, the electrical transient model in terms of the voltage and currents can be given in matrix form

$$\begin{bmatrix} v_{qs} \\ v_{ds} \\ v_{qr} \\ v_{dr} \end{bmatrix} = \begin{bmatrix} R_s + SL_s & \omega_e L_s & SL_m & \omega_e L_m \\ -\omega_e L_s & R_s + SL_s & -\omega_e L_m & SL_m \\ SL_m & (\omega_e - \omega_r) L_m & R_r + SL_r & (\omega_e - \omega_r) L_m \\ -(\omega_e - \omega_r) L_m & SL_m & -(\omega_e - \omega_r) L_r & R_r + SL_r \end{bmatrix} \begin{bmatrix} i_{qs} \\ i_{ds} \\ i_{qr} \\ i_{dr} \end{bmatrix} \quad (1.3)$$

There are basically two different types of vector control technique: direct and indirect vector control techniques. The direct implementation relies on the direct measurement or estimation of rotor stator or magnetizing-flux-linkage vector position and amplitude.

The indirect vector control method uses a machine model. For example, for the rotor flux oriented control, it utilizes the inherent slip relation. In contrast to direct methods, the indirect methods are highly dependent on machine parameters.

Traditionally, the direct vector control schemes use search coils, tapped stator windings or Hall Effect sensors for flux sensing. This introduces a limitation due to the machine structural and thermal requirements. Many applications, uses indirect schemes, since these have relatively simpler hardware and better overall performance at low frequencies, but since these contain various parameters, which may vary with temperature, saturation level and frequency. Various parameter adaptation schemes, has been developed. These include model reference adaptive system (MRAS) applications, self tuning control application, applications of observers, and applications of intelligent controllers etc. to obtain solutions. It is sometimes assumed that, mechanical time constant is greater than the electrical time constants, but this becomes an invalid assumption, if the machine inertia is low. If incorrect modulus and angle of the flux linkage space vector are used in a vector control scheme, then the flux and the torque decoupling is lost and the transient and steady state responses are degraded. Low frequency response, speed oscillations, and loss of input output torque linearity is a major consequence of detuned operation, together with decreased drive efficiency.

1.4.4 dq-abc Transformation

The relation between stationary reference frame and synchronously rotating reference frame is derived by reverse Park's transformation.

$$\begin{bmatrix} i_a \\ i_b \\ i_c \end{bmatrix} = \begin{bmatrix} \cos\theta & -\cos\theta \\ \cos\left(\theta_e - \frac{2\pi}{3}\right) & -\sin\left(\theta_e - \frac{2\pi}{3}\right) \\ \cos\left(\theta_e + \frac{2\pi}{3}\right) & -\sin\left(\theta_e + \frac{2\pi}{3}\right) \end{bmatrix} \begin{bmatrix} i_d \\ i_q \end{bmatrix} \quad (1.4)$$

Where, θ_e denotes the position of an angle between *d*-axis and *a*-axis of the synchronously rotating reference frame and stationary reference frame respectively [1]. The advantage of this state transformation in this new reference frame is that, the electromagnetic torque is directly an image of the quadrature ("q") component of stator current.

1.4.5 Direct or Feedback Vector Control

Let us consider synchronously rotating reference frame, where the principal vector control parameters, i_{ds}^* and i_{qs}^* are the dc values are converted into a stationary reference frame. The phase current commands for the inverter which are produced from the stationary reference frame signals. With the help of a voltage model estimator the flux signals Ψ_{dr}^s and Ψ_{qr}^s are generated from the machine terminal voltages and the currents. The flux control loop is added for a precision control of i_{ds}^* and the torque component of current $i_{qs}^*$is generated from the speed control loop with a bipolar limiter. Therefore, the torque produced is proportional to i_{qs}, can be a bipolar.

The correct alignment of current i_{ds} in the direction of the flux, $\hat{\Psi}_r$ and the current i_{qs} *is* perpendicular to it , are explained with the help of a rotor flux vectors Ψ_{dr}^s and Ψ_{qr}^s in the stationary reference frame as shown in Fig 1.4. In Figure, we see that, the $d^e - q^e$frame is rotating with synchronous speed ω_e, with respect to the stationary reference frame $d^s - q^s$, and at any instant, the angular position of $d^e - q^e$to $d^s - q^s$ axis is θ_e.

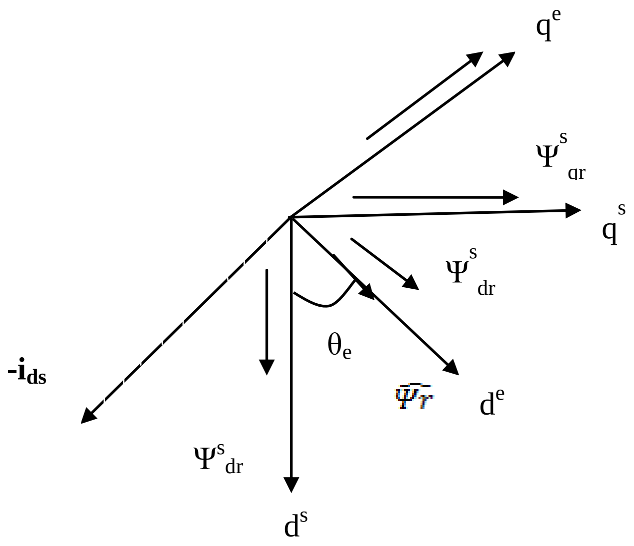

Fig 1.6 $d^s - q^s$ and $d^e - q^e$ phasors with correct rotor flux orientation

From Fig 1.6 we can write the following equations:

$$\Psi^{s}_{dr} = \hat{\Psi}_{r} \cos\theta_{e} \tag{1.5}$$

$$\Psi^{s}_{qr} = \hat{\Psi}_{r} \sin\theta_{e} \tag{1.6}$$

$$\cos\theta_{e} = \frac{\Psi^{s}_{dr}}{\hat{\Psi}_{r}} \tag{1.7}$$

$$\sin\theta_{e} = \frac{\Psi^{s}_{qr}}{\hat{\Psi}_{r}} \tag{1.8}$$

$$\hat{\Psi}_{r} = \sqrt{\Psi^{s^2}_{dr} + \Psi^{s^2}_{qr}} \tag{1.9}$$

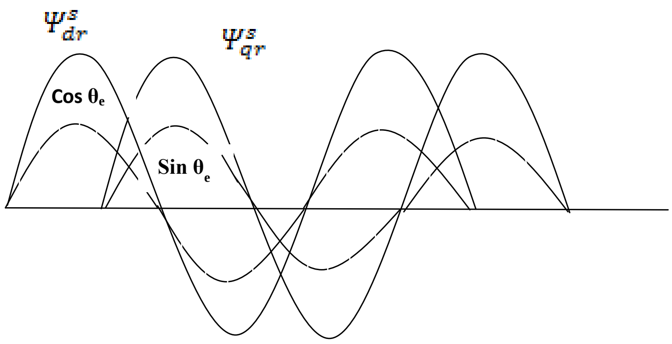

Fig 1.7 Plot of unit vector signals in correct phase positions

Let us now summarize some salient features of vector control

- In case of vector control the frequency ω_e of the drive is not directly controlled as in scalar control. The machine said to be a self-controlled, where the phase, as well as the frequency is indirectly controlled by a unit vector.
- In vector control there is no problem of instability, in crossing the operating point beyond the breakdown torque T_{em}, which is in a scalar control.

- As in vector control, the torque is control by the i_{qs} current and it does not affect the flux. Due to that, we get fast transient response, like a dc machine. The ideal vector control is not possible, Because of signal processing, parameter variations effect and delays in converter.
- Speed control is possible in all four quadrants without any control elements like reversing of phase sequence. In forward motoring mode, if torque T_e becomes negative, initially the drive goes to regenerative braking mode, which slows down the speed. The phase sequence of the unit vector automatically reverses at zero speed, and giving a reverse motoring operation.

The direct or feedback method of vector control is difficult to operate at low frequency including zero speed, due to the following problems:

- The voltage signals v_{ds}^{s} and v_{qs}^{s} are very low, at a low frequency; therefore the integration becomes difficult because of the dc offset trends build up at the integrator output.
- The effect of parameter variation of resistance R_s and inductance L_{ls}, L_{lr} and L_m reduce the accuracy of the estimated signals. The variation of resistance with temperature becomes more dominant and at higher voltages the effect of parameters variations can be neglected.

Direct vector control method with voltage signal estimation not used in industrial applications, because vector control drives operating from zero speed (including zero speed start up).

1.4.6 Indirect (Feed Forward) Vector Control

The indirect vector control method is same as the direct vector control, the only difference is the unit vector signals are generated in a feed forward manner in indirect vector control. In industrial applications Indirect vector control is much popular as compared to direct vector control. The fundamental principle of the indirect vector control is explained with the help of given phasor diagram as shown in Fig 1.8.

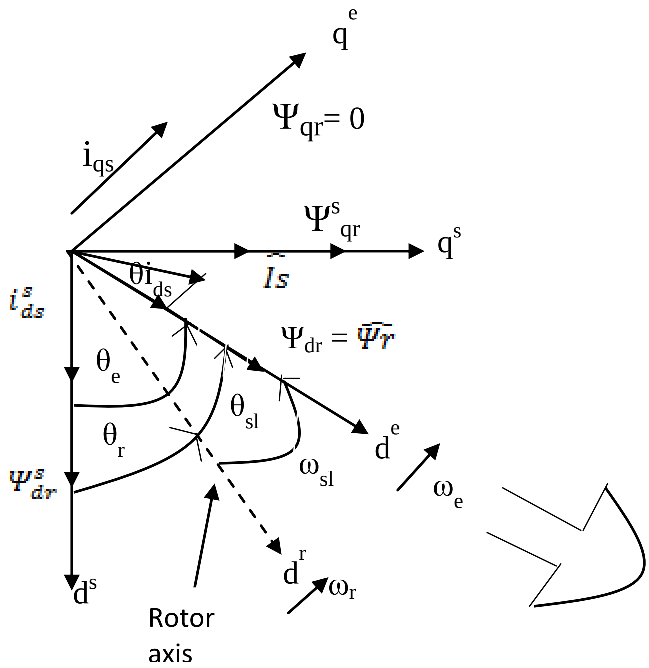

Fig 1.8 Phasor diagram explaining indirect vector control

The $d^r - q^r$ axes which are fixed on rotor, are moving with speed ω_r, where as $d^s - q^s$ axes are fixed on stator, as shown in the Fig 1.8. The synchronously rotating axes $d^e - q^e$ are rotating ahead of the $d^r - q^r$ axes by positive slip angle θ_{sl} corresponding to slip frequency ω_{sl}.

$$\omega_e = \omega_r + \omega_{sl} \tag{1.10}$$

We can write,

$$\theta_e = \int \omega_e dt = \int (\omega_r + \omega_{sl})\, dt = \theta_r + \theta_{sl} \tag{1.11}$$

The position of rotor pole is slipping with respect to the rotor at frequency of ω_{sl}. The stator flux component of current i_{ds} should be aligned on the d^e axis, and the torque component of current i_{qs} on the q^e axes as shown in the Fig 1.8.

From the voltage model of the flux vector estimation, the machine terminal voltage and the current is sensed and fluxes are computed from stationary reference frame $d^s - q^s$ equivalent circuits. The flux equations are given as:

$$\Psi^s_{ds} = \int (v^s_{ds} - R_s i^s_{ds})dt \tag{1.12}$$

$$\Psi^s_{qs} = \int (v^s_{ds} - R_s i^s_{ds})dt \tag{1.13}$$

$$\Psi_r^{s\,2}=\Psi_{dr}^{s\;2}+\Psi_{qr}^{s\;2} \qquad (1.14)$$

$$\Psi_{dm}^{s}=\Psi_{ds}^{s}-L_{ls}i_{ds}^{s} \;=\; L_m\left(i_{ds}^{\;2}+i_{dr}^{\;2}\right) \qquad (1.15)$$

$$\Psi_{qm}^{s}=\Psi_{qs}^{s}-L_{ls}i_{qs}^{s} \;=\; L_m\left(i_{qs}^{\;2}+i_{qr}^{\;2}\right) \qquad (1.16)$$

$$\Psi_{dr}^{s}=L_m i_{ds}^{s}+L_r i_{dr}^{s} \qquad (1.17)$$

$$\Psi_{qr}^{s}=L_m i_{qs}^{s}+L_r i_{qr}^{s} \qquad (1.18)$$

Eliminating i_{dr}^{s} and i_{qr}^{s} from equations 1.17 and 1.18 with the help of the equations 1.15 and 1.16 respectively,

Therefore we get,

$$\Psi_{dr}^{s} = \frac{\mathrm{Lr}}{\mathrm{Lm}}\Psi_{dm}^{s} - L_{lr}i_{ds}^{s} \qquad (1.19)$$

$$\Psi_{qr}^{s} = \frac{\mathrm{Lr}}{\mathrm{Lm}}\Psi_{qm}^{s} - L_{lr}i_{qs}^{s} \qquad (1.20)$$

For decoupling control, we make a derivation for the control equations of indirect vector control using equivalent circuits. The rotor circuit equations written as.

$$\frac{d\Psi\mathrm{dr}}{dt} + R_r i_{dr} - (\omega_e - \omega_r)\Psi_{qr} = 0 \qquad (1.21)$$

$$\frac{d\Psi\mathrm{qr}}{dt} + R_r i_{qr} + (\omega_e - \omega_r)\Psi_{dr} = 0 \qquad (1.22)$$

The equations for rotor flux linkage can be given as

$$\Psi_{dr} = L_r i_{dr} + L_m i_{ds} \qquad (1.23)$$

$$\Psi_{qr} = L_r i_{qr} + L_m i_{qs} \qquad (1.24)$$

With the help of above equations we can write as

$$i_{dr} = \frac{1}{\mathrm{Lr}\,\Psi\mathrm{dr}} - \frac{\mathrm{Lm}}{\mathrm{Lr\,ids}} \qquad (1.25)$$

$$i_{qr} = \frac{1}{\mathrm{Lr}\,\Psi\mathrm{qr}} - \frac{\mathrm{Lm}}{\mathrm{Lr\,iqs}} \qquad (1.26)$$

With the help of equations 1.25 and 1.26, the equations 1.21 and 1.22 can be written as

$$\frac{d\Psi dr}{dt} + \frac{Rr}{Lr}\Psi_{dr} - \frac{Lm}{Lr}R_r i_{ds} - \omega_{sl}\Psi_{qr} = 0 \qquad (1.27)$$

$$\frac{d\Psi qr}{dt} + \frac{Rr}{Lr}\Psi_{qr} - \frac{Lm}{Lr}R_r i_{qs} - \omega_{sl}\Psi_{qr} = 0 \qquad (1.28)$$

Where,

$\omega_{sl} = \omega_e - \omega_r$ is substituted, for decoupled control, therefore it is desirable that

$$\Psi_{qr} = 0 \qquad (1.29)$$

$$\frac{d\Psi qr}{dt} = 0 \qquad (1.30)$$

So that, total rotor flux $\hat{\Psi}_r$ is directed on the d^e axis.

Substituting above conditions in equations 1.29 and 1.30, we get

$$\frac{Lm}{Lr}\frac{d\hat{\Psi}r}{dt} + \hat{\Psi}_r = L_m i_{ds} \qquad (1.31)$$

$$\omega_{sl} = \frac{LmRr}{\hat{\Psi}r\,Lr} i_{qs} \qquad (1.32)$$

Where,

$\hat{\Psi}_r = \Psi_{dr}$ is substituted

If the rotor flux $\hat{\Psi}_r$ = constants, then from equation 1.30

$$\hat{\Psi}_r = L_m i_{ds} \qquad (1.33)$$

Or we can say that, the current i_{ds} in steady state are directly proportional to rotor flux. If we implement the indirect vector control scheme, then the equations 1.11, 1.31 and 1.32 should be taken into considerations. The range of speed control in indirect vector control is extended from zero speed or stand still to field weakening region. In field weakening region, the flux is programmed, in such way so that the inverter is operated in PWM mode. The instantaneous current control of the inverter is necessary in both the direct and indirect vector control methods [1].

1.5 DIRECT TORQUE CONTROL

Direct Torque Control was first introduced by Takahashi in 1984 in Japan and by Dopenbrock in 1985 in Germany [3] after that this control scheme becomes the world's most advanced AC Drives control technology. DTC does not require any coordinate transformation, PI regulators, and Pulse width modulator and position encoders and because of that, it is called a simple control technique. In DTC there is a direct and independent controlled of motor torque and flux by selecting optimum inverter switching modes. The electromagnetic torque and stator flux are calculated from the motor inputs e.g. stator voltages and currents [16]. The voltage vector selection for the inverter is such that the torque and flux errors are within the hysteresis bands limits. The main advantages of DTC technique are quick torque response in transient condition and efficiency improvement in steady state. The Direct torque control (DTC) technique is one of the most actively researched control techniques where we can effectively control the torque and flux.

1.6 SENSORLESS CONTROL OF INDUCTION MOTOR DRIVES

Sensorless vector controlled IM drives are developed for better performance industrial drive systems. This type of control techniques decrease the cost drives, size and the maintenance requirements and increasing the reliability of the system, robustness and immunity to noise [4,6]. The using of a speed sensor is not practical in a hostile environment. Sensorless control has some disadvantages like Parameter sensitivity, high computational effort and instability at low and zero speed [7]. Therefore sensorless drives applied in medium and high speed regions. The main focus of the researchers is to extend the operating region of sensorless drives at near zero stator frequency [7, 8].There has been several methods for the rotor speed estimation in sensorless IM drives [4, 5]. Generally, these methods divided into two main categories: fundamental excitation and spectral analysis techniques [4]. Among the several methods proposed for sensorless IM drives, MRAS are the most popular technique employed for IM because of their smaller computational effort and simple implementation.

1.7 ORGANIZATION OF THESIS

Apart from the introduction chapter 1 contains introduction of IMD, types of control scheme, dynamic modeling of the induction motor such as scalar control, vector control and its principle, dynamic d-q model of the machine and the dc drive analogy to the induction machine and sensorless control of IM and estimation of stator resistance using MRAS. Chapter 2 contains the literature survey of the thesis. Chapter 3 contains voltage source inverter (VSI) its working and switching modes. Chapter 4 contains space vector pulse width modulation fed induction motor drives SVPWM theory and Pulse pattern generation. Chapter 5 describes the estimation techniques to estimate the speed without any sensor so called sensorless control and estimate the stator resistance using MRAS. Chapter 6 explains simulation model of sensorless IM drive and contains graphs of speed, torque, currents and stator resistance at different load conditions Chapter 7 contains finally the achievements, future work, research and conclusion is discussed.

1. 8 CONCLUSION

In this chapter the complete introduction of an induction machine theory has been presented. The different types of control scheme have been discussed like Scalar control, Vector control, direct torque control and Sensor-less control. Accordingly, representation of a two-axis state space of an IM in the stator frame reference also developed. In order to explain the principles of vector control strategy the equations of an induction machine, are expressed in the synchronous frame of reference has been used. This chapter also presented the some salient features of vector control. The different estimation technique used for the estimation of Rotor speed of an IM using MRAS approach has been presented. The space phasor notation is used to formulate the model two axis theory, as space phasor notation is compact and easier to work with. Finally, the design of an appropriate adaptation mechanism using hyperstability criterion has been demonstrated.

CHAPTER 2

LITERATURE REVIEW

2.1 INTRODUCTION

In the past, IM have been used mainly in constant speed applications because conventional methods are either expensive or highly inefficient. For variable speed applications dc drives were dominated. The main drawback of dc motors is the presence of commutator and brushes, because they require frequent maintenance and not suitable for dirty environments [1]. These shortcomings are overcome by induction motors, particularly squirrel-cage induction motor, as they require low maintenance, cheaper, lighter and can operate in dirty and explosive environments. Availability of power electronics devices, thyristors, IGBT and GTO results in the developments of variable speed induction motor drives. The variable induction motor drives are costly then dc drives and used in fans, blowers, cranes, conveyers, traction etc. because of advantages of IM. Due to this advancement in electronics during last decades has a result in large growth in automation of industrial processes.

2.2 DYNAMIC MODELING AND VECTOR CONTROL OF IM DRIVE

The idea of vector control of IM first came in the 1970's and has ever since revolutionized control of ac drives. Though, the common methods of control satisfied the objectives like v/f control, but gives poor performance to fast changing signals. Better performance of vector control of IM achieved by employing the transformation techniques. The transformation techniques enable the IM to be controlled by using the independent signals that controls the control variables. In vector control, the induction machine operates like a dc machine in the rotating dq frame or we can say that the IM quantities appear as dc quantities. The stator d-q axis components, i_{ds} and i_{qs} are used to control the rotor flux and the torque respectively and there is independent control of torque and flux in the machine [10]. The dc signal in the rotating d-q frame is easy to control with the help of proportional integral (PI) controllers. For better accuracy, it should be a accurate control of i_{ds} and $i_{qs,}$ and accurate estimation of rotor flux position. The position of rotor flux allows the transformation of quantities from rotating reference frame to stationary reference frame. On the basis of method used for estimation of rotor flux position, vector control is classified into direct vector control and indirect vector control as per [11]. Earl C. Barnes [12] reported the performance and characterstics of IM motors with solid – state variables frequency drives. Trevor L. Grant et al. [13] reported the operation PWM based drives in three distinct modes, viz pure PWM at the lower speeds pure six – step at the higher speeds, and quassi- PWM at the intermediate speeds, with insights into the Bessel approximation to the PWM waveform. Comparison of different PWM-VSI fed 3 Φ IM based on modulation index and switching frequency are investigated by Bikram Das et.al. [14]. Development and Comparative Analysis of a Pulse-Width Modulation Strategy is reported by Marlen Varnovitsky [15]. Jie Zhang [16] reported the primary current vector control of a CSI fed IMD with an improved estimation of slip angular frequency. A high performance control of squirrel cage IM drive fed by a three – level IGBT inverter operating at a low switching frequency is reported by Jie Zhang [17].

Power electronic devices like ASDs include power converters, control elements and electric machines made from linear and non linear elements and semiconductor devices. Such systems require some software applications for the simulation and modelling. For that there are some simulation tools which categorized into simulation programs like EMTP, SPICE-based simulation programs etc. and simulation software like Matlab/simulink etc. Adel Aktaibi et al. [18] presented the dynamic simulation model of a three phase IM step by step using dq0 axis transformations of the stator and rotor variables in arbitrary reference frame. Leonhard, W and Vas.P [19, 20] presented the induction motor model in stationary reference frame. Modelling analysis and simulation of induction motor drive using conventional, PI, Fuzzy Controller in open loop and closed loop have been presented by P.M Menghal et.al. [21]. Raad S.Fayath et.al. [22]. presented the methodology for modeling of IFOC induction motor drive system. In which the differential equation are used to represent the numerical model of squirrel cage IM. Scott Wade et al. [23, 24] presented the simulation model of vector controlled induction machine system using a linear supply and a PWM supply, where an Extended Kalman based parameter identification algorithm is used for rotor resistance estimation. K. L. Shi et. al. [25] presented a paper that explained the model of a 3-phase IM and its simulation using Matlab/Simulink including constructional details of various sub-models Simulink implementation of an IM model is presented by Burak Ozpineci in 2003 [26]. Saffet Ayasun et al. [27] presented MATLAB/Simulink implementation of no-load test and a blocked rotor test performed to identify equivalent circuit parameters of IM. The simulation of induction motor frames is presented in this paper. The voltage, torque and current waveforms are included in the comparison of the induction motor frames presented by K.S. Graeid et.al. [28]. O. D. Momoh et. al. [29] presented somewhat different induction machine model equations in which flux linkage equations are expressed in terms of reactance rather than inductances is used.

2.3 SPEED AND RESISTANCE ESTIMATION TECHNIQUES

In the last three decades control of high performance IM drive has been an active area of research and there has many control techniques have been evolved for the torque and speed control of induction motor drives. The major areas of research in control schemes include open loop and closed loop v/f control, vector or field oriented control, direct torque control, sensor-less control. Model reference adaptive system (MRAS) is an adaptive control technique used for speed estimation and resistance estimation of sensor-less IM drive.

Various MRAS observers have been introduced in the literature, depending upon the output states that form the error function presented by Shady Mostafa Gadoue. For speed control of IM an accurate estimation of rotor flux is required, which can be estimated by the rotor or the stator variables. A scheme is presented by L.Umanand et.al. [30] for online estimation of stator resistance for various speed control applications under steady state operating conditions. A.M .El-Sawy et.al presented a parallel estimation of speed and stator resistance based on MRAS scheme of IM drives along with an online estimation of magnetizing inductance has been used within the speed estimator. Digital simulations also carried out to evaluate the effectiveness of proposed sensor-less drive system [31]. Cherifi Djamila et.al [32] has a continuing research on the elimination of the problem of sensitivity. They presented a simple method for the simultaneous estimation of stator resistance and rotor speed in sensorless IFOC of IM drive using a luenberger observer and stability of this observer is proved by lyapunov’s theorem. The feasibility of luenberger observer is verified by simulation. Ahmad Razani et.al [33] represents the MRAS scheme to estimate the speed of an IM by two different approach, RF-MRAS and BEMF-MRAS

The online estimation of stator resistance in vector control of IM drives directly from decoupled stator variables via reactive power measurements is presented by B. Mouli Chandra et.al [34]. C. Chakraborty et.al. [35] presented a new V x I Adaptive Speed Sensor less four quadrant vector controlled induction motor drive. The speed estimator utilizes instantaneous and steady state values of voltages and current for estimation of speed and stator resistance in the reference and adjustable models of the MRAS respectively at low speed or zero speed. V. Vasic et.al [36] reported a stator resistance estimation technique for speed sensor-less rotor flux oriented IMD. A.V Ravi Teja.et.al [37] describes a new model reference adaptive system for four quadrant vector control induction motor drive. Aswathy Vijay et.al. [38] presented a MRAC estimation technique for the estimation of stator resistance of a sensorless IMD. Colin Schauder [39] presented a model-reference adaptive system (MRAS) for the estimation of IM speed from terminal voltages and currents implemented on a 30 hp drive. Geng Yang et.al. [40] described a MRAS technique for speed control of the vector controlled sensor-less IM drive. The paper presented by Min-Huei Kim et.al.[42] reported a vector control system based on MRAS for a sensor-less IM operating at very low speed. [43] On-line estimation of rotor resistance in a vector controlled IM is presented by Scott Wade et.al. Induction motor (IM) speed sensorless control, allowing operation at low speed and zero speed, optimizing torque response and efficiency, will be presented in G. Edelbaher et.al. [44]. Paul C. Krause et.al. [45] presents classical techniques used to establish the voltage and torque equations for asymmetrical induction machine expressed in terms of machine variables and the modification of the transformation to arbitrary reference frame to accommodate rotating circuits. This paper described an artificial neural network (ANN) based adaptive estimator for the estimation of rotor speed in a sensorless vector- controlled induction motor (IM) drive. The model reference adaptive system (MRAS) is formed with instantaneous and steady state reactive power. A stable MRAS speed estimator based on current estimation is proposed in this paper. The MRAS based on flux estimation scheme suffers from the problems of using pure integration. On the other hand, those based on back-EMF or on current estimation become unstable in the generating mode of operation due to incomplete satisfaction of stability conditions, especially at low speeds presented by M. Rashed et.al. [48]. R. J. Kerkman et.al. [49] presented a new technique-the back electromagnetic force (BEMF) detector-for reducing the adverse effects of stator resistance on field oriented control is presented and evaluated through simulation and experimental results. I. J. Ha et.al. described an online identification method for both stator and rotor resistance of induction motors without rotational transducers [51]. M. Cirrincione [53] presented a paper of Sensor-less control of induction machines by a new neural algorithm. M. Tsuji et.al [54] presents a sensorless vector control system for general-purpose induction motors, based on the observer theory and the adaptive control theories. The proposed system includes a rotor speed estimator using a q-axis flux and stator resistance identifier using the d-axis flux. [55] K. Akatsu et.al. described a Sensorless very low-speed and zero speed estimations with online rotor resistance estimation of induction motor without signal injection. R. Marino et.al. represent an On-line stator and rotor resistance estimation for induction motor [57]. S. Maitiand [58] presented a new instantaneous reactive power based MRAS for sensor less induction motor drive. [61] Ashutosh Mishra et.al. explained the Speed Control of An IM by using indirect vector control method. G. Pydiraju et.al, described the Sensorless Speed Control of Induction Motor Using MRAS [62]. Zhifeng Zhang, Renyuan Tang, discuused a novel Direct Torque Control Based on Space Vector With Modulation Adaptive Stator Flux Observer for Induction Motors [66].

2.5 CONCLUSION

This chapter has provided a detailed review of different model based techniques applied to speed sensorless IM drives with most emphasis given to MRAS. Different problems affecting the low speed operation of MRAS observers have been illustrated. Various methods employed in the literature for the estimation of speed and stator resistance. It appears that, despite much attempt and progress, operation at very low speed for MRAS-based sensorless IM drives is still challenging and needs more investigation.

CHAPTER 3

VOLTAGE SOURCE INVERTER FED INDUCTION MOTOR DRIVES

3.1 INTRODUCTION

For providing adjustable-frequency power to industrial applications, three phase inverters are commonly used. Three phase inverters like single phase inverters, take their dc supply from a battery or usually from a rectifier. On the basis of the type of an ac output waveform, the power converter topologies are considered to be voltage source inverters (VSIs) where the ac output is a voltage waveform. and similarly for the current source inverters (CSIs) the output is a current waveform.

These structures are widely used because they are required by many industrial applications because of their naturally behaviour as a voltage sources, such as adjustable speed drives (ASDs). The three phase induction motor is driven by voltage source inverter (VSI), which is further connected to the load of the drive system.

3.2 AXES TRANSFORMATION

Two axis theory has been used for dynamic modeling of the motor [1]. According to this theory the time varying parameters can be expressed in direct (d-axis) and quadrature (q-axis) axis, which are mutually perpendicular to each other. For the representation of the d-q model of the machine a stationary or rotating reference frame is assumed.

3.2.1 Three phase to two phase transformation

Let us considered a symmetrical three phase machine with stationary *as-bs-cs* axes which is at 120 degree apart as shown in Fig.3.1

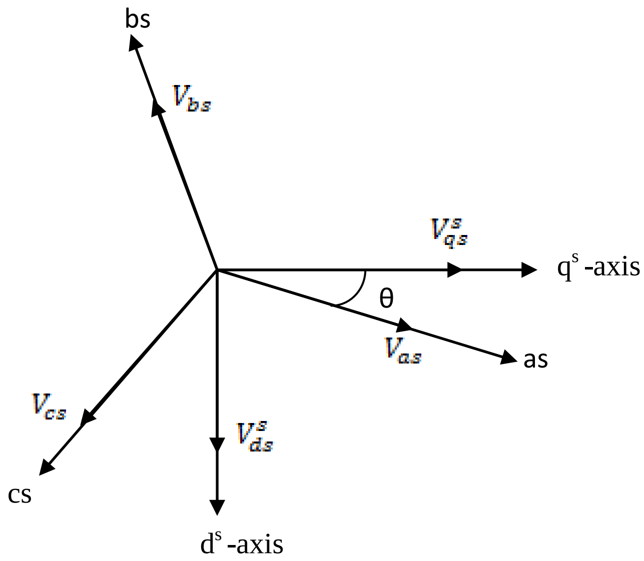

Fig.3.1 Stationary frame a-b-c to ds-qs axes transformation

The voltages $v_{as}.v_{bs}.v_{cs}$ are the voltages of as, bs, cs phases respectively. Now assuming that the stationary d^s-q^s axes are oriented at θ angle as shown and the voltages along d^s-q^s axes to be v_{ds}^s, v_{qs}^s respectively, the stationary two phase voltages can be transformed to three phase voltages according to the following equation:

$$v_{as} = v_{qs}^s \cos\theta + v_{ds}^s \sin\theta \tag{3.1}$$

$$v_{bs} = v_{qs}^s \cos(\theta - 120) + v_{ds}^s \sin(\theta - 120) \tag{3.2}$$

$$v_{cs} = v_{qs}^s \cos(\theta + 120) + v_{ds}^s \sin(\theta + 120) \tag{3.3}$$

The phase voltages in matrix form can be written as:

$$\begin{bmatrix} v_{as} \\ v_{bs} \\ v_{cs} \end{bmatrix} = \begin{bmatrix} \cos\theta & \sin\theta & 1 \\ \cos(\theta - 120) & \sin(\theta - 120) & 1 \\ \cos(\theta + 120) & \sin(\theta + 120) & 1 \end{bmatrix} \begin{bmatrix} v_{qs}^s \\ v_{ds}^s \\ v_{0s}^s \end{bmatrix} \tag{3.4}$$

By inverse transformation, v_{ds}^s and v_{qs}^s can be written in terms of three phase voltages in matrix form as follows:

$$\begin{bmatrix} v_{qs}^s \\ v_{ds}^s \\ v_{0s}^s \end{bmatrix} = \begin{bmatrix} \cos\theta & \cos(\theta - 120) & \cos(\theta + 120) \\ \sin\theta & \sin(\theta - 120) & \sin(\theta + 120) \\ 0.5 & 0.5 & 0.5 \end{bmatrix} \begin{bmatrix} v_{as} \\ v_{bs} \\ v_{cs} \end{bmatrix} \tag{3.5}$$

Where v_{0s}^s is a zero sequence component which may or may not be present. If q^s-axis aligned with the as-axis i.e. $\theta = 0$ then the zero sequence component is neglected and the transformation relations are reduced to:

$$v_{as} = v_{qs}^{s} \quad (3.6)$$

$$v_{bs} = -\frac{1}{2}v_{qs}^{s} - \frac{\sqrt{3}}{2}v_{ds}^{s} \quad (3.7)$$

$$v_{cs} = -\frac{1}{2}v_{qs}^{s} + \frac{\sqrt{3}}{2}v_{ds}^{s} \quad (3.8)$$

$$v_{qs}^{s} = v_{as} \quad (3.9)$$

$$v_{ds}^{s} = -\frac{1}{\sqrt{3}}(v_{bs} - v_{cs}) \quad (3.10)$$

3.2.2 Two phase stationary to two phase synchronously rotating frame transformation

The transformation of stationary $d^{s} - q^{s}$ axes to synchronously rotating $d^{e} - q^{e}$ reference frame, rotating at speed of ω_{e} with respect to $d^{s} - q^{s}$ axes as shown in Fig.3.2. The angle between the and d^{e} axes is $\theta_{e} = \omega_{e}$ t. The voltages v_{ds}^{s} and v_{qs}^{s} are converted to voltages on $d^{e} - q^{e}$ axis as shown below:

$$v_{ds} = v_{qs}^{s}\cos\theta_{e} - v_{ds}^{s}\sin\theta_{e} \quad (3.11)$$

$$v_{qs} = v_{qs}^{s}\sin\theta_{e} + v_{ds}^{s}\cos\theta_{e} \quad (3.12)$$

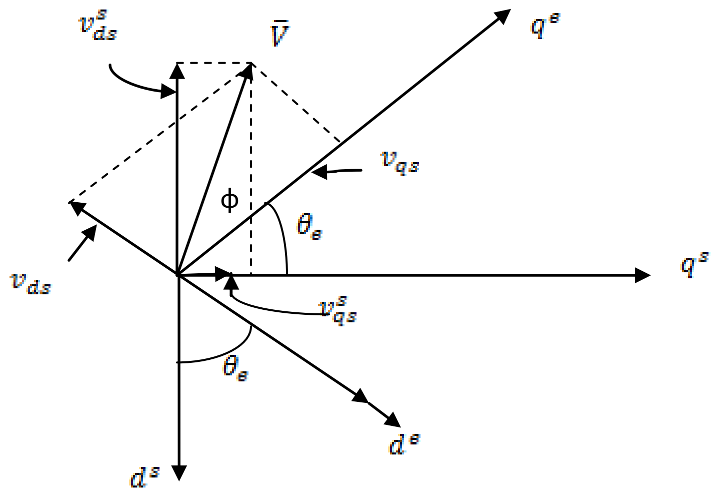

Fig.3.2 Stationary d^{s}-q^{s} frame to synchronously rotating frame d^{e}-q^{e} transformation

The transformation of parameters from rotating reference frame to stationary reference frame can be done according to the following relations:

$$v_{qs}^{s} = v_{qs}\cos\theta_{e} + v_{ds}\sin\theta_{e} \quad (3.13)$$

$$v_{ds}^{s} = -v_{qs}\sin\theta_{e} + v_{ds}\cos\theta_{e} \quad (3.14)$$

Assumed that the three phase voltages are balanced and sinusoidal and given as:

$$v_{as} = V_m \cos(\omega_e t + \varphi) \tag{3.15}$$

.

$$v_{bs} = V_m \cos(\omega_e + \varphi - \tfrac{2\pi}{3}) \tag{3.16}$$

$$v_{cs} = V_m \cos(\omega_e t + \varphi + \tfrac{2\pi}{3}) \tag{3.17}$$

Substitute the equations (3.15)-(3.17) in equations (3.10) and (3.11) and we get

$$v_{qs}^{s} = V_m \cos(\omega_e t + \varphi) \tag{3.18}$$

$$v_{ds}^{s} = - V_m \sin(\omega_e t + \varphi) \tag{3.19}$$

Substituting (3.18) – (3.19) in equation (3.11)-(3.12)

$$v_{qs} = V_m \cos\varphi \tag{3.20}$$

$$v_{ds} = - V_m \sin\varphi \tag{3.21}$$

From the equations (3.20) and (3.21) we see that the sinusoidal quantities in a stationary reference frame appear as dc quantities in a synchronously rotating reference frame.

3.3 VOLTAGE SOURCE INVERTER

In a voltage source inverter (VSI), the input voltage is set to be a constant and the amplitude of the output voltage does not depend on the nature of the load. Whereas the output waveform of the current and the magnitude is dependent on the nature of the load impedance. As compared to the single phase inverters the, three phase VSIs are commonly used in providing the adjustable frequency power to the industrial applications.

A basic three phase VSI is a six step bridge inverter with minimum six power electronics switches (i.e. IGBTs, Thyristors) and a six feedback diodes. A step is related to the firing angle and can be defined as, the change in firing from one switch to the next switch in proper sequence. In a six step inverter the step is of 60º interval for the complete cycle of 360º, means the switches would be operated at regular intervals of 60º in a proper sequence to get the three phase ac output voltage. The power circuit diagram of a three phase VSI as shown in Fig.2.5 which is mainly consist of six diodes and six IGBTs, where the diodes are connected in anti-parallel to the IGBTs.In order to maintain the input dc voltage constant, the capacitor is connected at the terminals. If there is any harmonics in the circuit this capacitor also suppresses them.

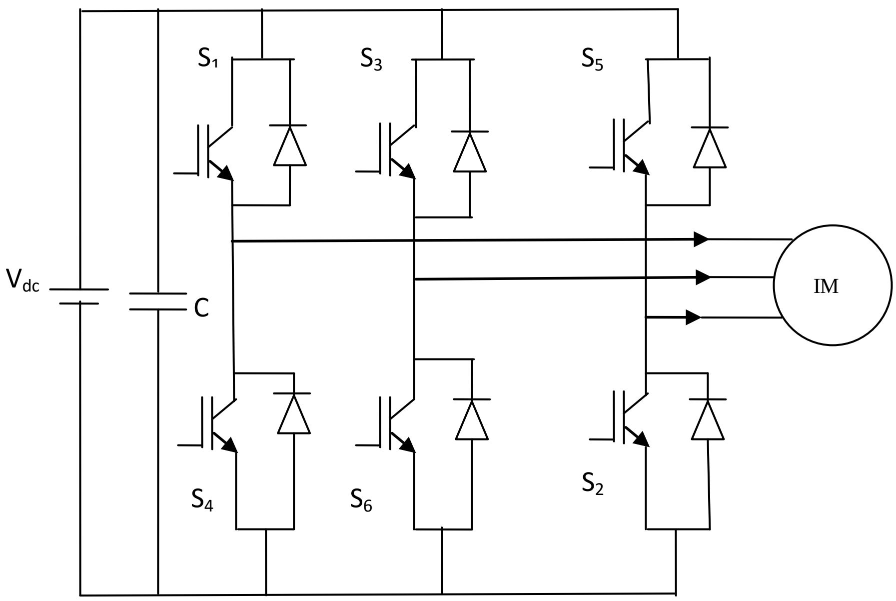

Fig. 3.3 Three phase VSI using IGBTs

For proper operation of VSIs the six switches are divided into two parts; both parts contains three switches each. The upper part has three switches called as positive group (i.e. S_1 , S_3 , S_5) and lower part also has three switches as negative group of switches (i.e. S_4, S_6 , S_2).. There are two conduction modes:

1. 180º conduction mode
2. 120º conduction mode.

3.3.1 Three phase 180 Degree Mode and 120 Degree Mode VSI

There are two gating patterns and in each pattern the gating signals are applied and removed at an interval of 60º of the output voltage waveform. In 180º conduction mode there are three switches, which are on at a time, two switches from a positive group and one switch from a negative group or vice versa as shown in Figure 3.4. The conduction period for each switch is 180º of a cycle. In 120º conduction mode each switch conduct for 120º in one cycle and rest of the two switches are turned on at a time i.e one from positive group and one from the negative group.

The two switches of the same leg cannot be turned on simultaneously in both case because it would short circuit the dc source as shown in Figure 3.5.

In 120º conduction mode there is no chances of short circuit of the dc link voltage source because each switch is conduct for 120º in one cycle and there is an interval of 60º in each cycle when no one switch is conducted and the output voltage is zero at this time interval. In other words we can say that there is a 60º interval gap between the turning off one switch and turning on of complimentary switch in the same leg. This interval is sufficient to regain its forward blocking capability of the outgoing switch.

3.3.2 Merits and Demerits of 120 degree mode over 180 degree mode inverter

In 180 degree mode inverter, when gate signal i_{g1} is cut-off to turn off S_1 at $\omega t = 180^0$, signal i_{g4} is simultaneously applied to turn on S_4 in the same leg. There is a commutation interval must exist between the removal of i_{g1} and application of i_{g4}, because otherwise dc source would experience a direct short circuit through S_1 and S_4 in the same leg.

This difficulty is overcome in 120 degree mode inverter, because there is a 60 degree phase difference between the turning off of S_1 and turning on of S_4. During this 60 degree interval, S_1 can be commutated safely.

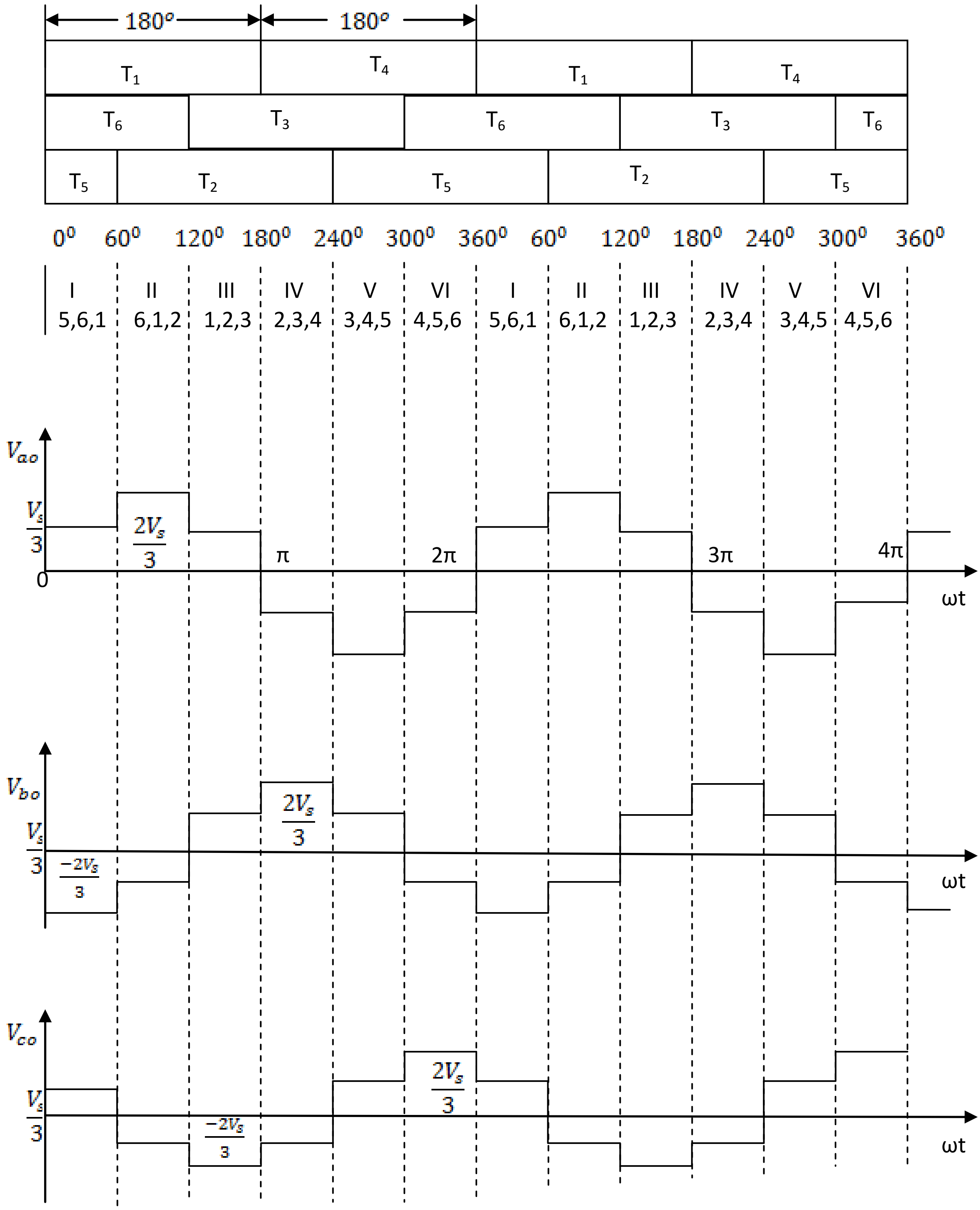

Fig. 3.4 Voltage waveform for 180° mode 3 - phase VSI

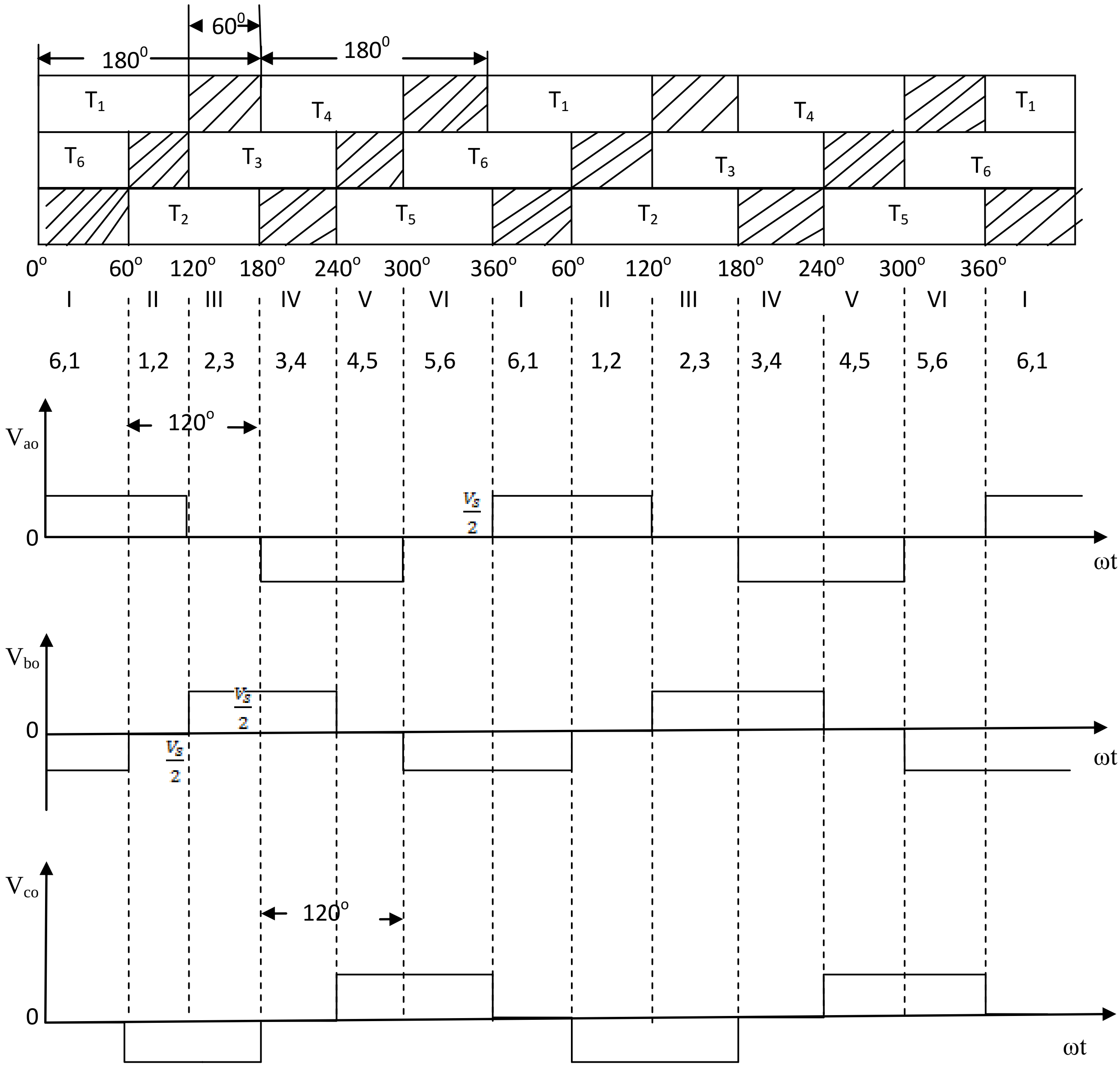

Fig. 3.5 Voltage waveform for 120° mode six-step 3-phase VSI

3.3.3 Switching States

A three-phase bridge inverter, as shown in the Figure 3.3, has 2^3 = 8 switching states. The Table-I gives a detail of the switching states and the corresponding phase to neutral voltage of a machine. Consider, for example, state 1, when switches Q_1, Q_6 and Q_2 are closed. In this state, phase a is connected to the positive terminal and phases b and c are connected to the negative terminal. The solution of the circuit indicates that $v_{an} = \frac{2}{3}V_d$, $v_{bn} = \frac{-1}{3}V_d$ and $v_{cn} = \frac{-1}{3}V_d$. The inverter has 6 active states (1-6) when voltage is impressed across the load, and two zero states (0 and 7) when the machine terminal are shorted through the lower devices or upper devices, respectively as shown in Table 3.1

Table 3.1 Switching states of a three phase VSI

State	On devices	V_{an}	V_{bn}	V_{cn}	Vector
0	$Q_4Q_6Q_2$	0	0	0	V_0 (000)
1	$Q_1Q_6Q_2$	$\frac{2V_d}{3}$	$\frac{-V_d}{3}$	$\frac{-V_d}{3}$	V_1 (100)
2	$Q_1Q_3Q_2$	$\frac{V_d}{3}$	$\frac{V_d}{3}$	$\frac{-2V_d}{3}$	V_2 (110)
3	$Q_4Q_3Q_2$		.		V_3 (010)
4	$Q_4Q_3Q_5$		.		V_4 (011)
5	$Q_4Q_6Q_5$		.		V_5 (001)
6	$Q_1Q_6Q_5$		.		V_6 (101)
7	$Q_1Q_3Q_5$	0	0	0	V_7 (111)

3.4 CONCLUSION

In this chapter the detail dynamic model of an IM is discussed in the synchronously rotating reference frame. To understand and design the vector controlled of an induction motor drives, the dynamic model of the machine to be controlled must be known which could be a good approximation of the real plant. To compute the model, the two axis theory and space phasor have been used. It has been proved that space phasor notation is compact and easier to work with. The supply to IM drive is given with the help of VSI. The complete working of VSI is explained in this chapter.

CHAPTER-4

SPACE VECTOR PULSE WIDTH MODULATION FED INDUCTION MOTOR DRIVES

4.1 INTRODUCTION

The use of a PWM is an advantageous to machine drives in many ways like it has the ability to run the motor with a sinusoidal waveform of a current and very helpful in obtaining a dc input through uncontrolled rectification of AC mains and it has a very high efficiency, a good power factor and relatively free from regulation problems. In case of a open loop control system, the conventional PWM techniques are very suitable. Whereas space vector PWM (SVPWM) technique is very suitable for the implementation of closed loop controlled AC drive system. The switching patterns of the bridge inverter in case of SVPWM technique are generated from the stator voltage space phasor. A reference voltage vector is generated by utilizing different switching states of the three phase bridge inverter in order to generate the field which is synchronous with the rotating voltage vector.

4.2 THEORY OF SPACE VECTOR PULSE WIDTH MODULATION

When a three phase input supply is given to the stator of an induction motor, a rotating magnetic field is produced which is also in three phase. As a result, a field flux of three phase rotating voltage vector is generated, which lags the flux by 90º. This field can also be realized by a logical combination of the inverter switching which is the basic concept of SVPWM.

4.2.1 Realization of voltage space phasor

There are total of eight switching states are possible in the three phase bridge inverter in which two states are zero states and the six states are active states and has a well-defined ON or OFF state in each configurations. The switching is done in such a way that only one switch is operate (ON) in each of the three legs at a particular instant. Corresponding to each state of inverter, there is only one voltage space vector. It can be explained as, let us assume that, for a zero state it has voltage space vector V_0 , and for state 1 it has V_1 voltage space vector and so on. The magnitude of these voltage switching state vectors is equal, but 60º apart from each other. These state vectors can be written as :

$$V_k = V_{dc}\ e^{j\left(\frac{k-1}{3}\right)\pi} \qquad k = 1,2,\ldots\ldots\ldots 6$$

$$= 0 \qquad k\ 0,7 \qquad (4.1)$$

Where, k = inverter state number.

V_{dc} = dc link voltage of the inverter

The Fig 4.1 shows the inverter state vectors.

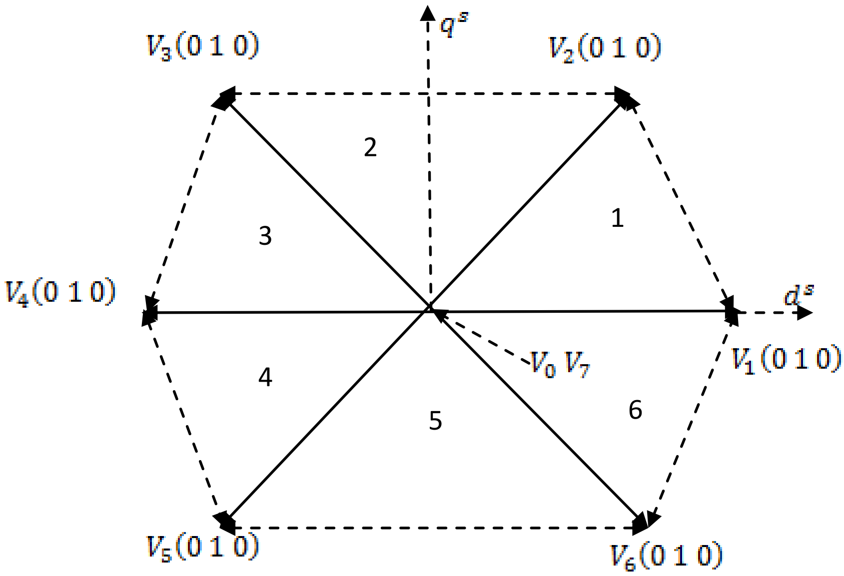

Fig. 4.1 Inverter switching state vectors

The above Fig 4.1 shows the plane which is divided into six equal sectors with each sector is of 60º apart and the space bounded by two inverter space vectors is called a sector. These voltage vectors are 120º apart in space are represented by the rotating vectors, in case of balanced three phase system. The projections of these vectors are sinusoidal on the fixed three phase axes and they can be represented by a voltage reference space vector V_{ref}^* or V_s^* by the three sinusoidal references.

The rotation of the reference vector is assumed to rotated through the six sectors in anti-clockwise direction with respect to the d^s-axis as shown in Fig.4.2. At switching instant t_s the combination of eight state vectors can synthesized the reference space vector having a constant magnitude. In this case the output frequency is much lower than the switching frequency. These states are valid only for certain amount of time.

$$V_s^* = V_k t_k + V_{k+1} t_{k+1} \qquad k = 0, 1, 2\ldots\ldots, 7 \qquad (4.2)$$

The space phasor of stator voltage V_s^*, in SVPWM, is assumed to be moving in a circular path in a $d^s - q^s$ plane with constant angular velocity. The basis of SVPWM scheme is to sample the stator voltage V_s^* at higher rate, between the sampling instants, and the vector is assumed to be constant in magnitude which is as shown in Fig. 4.2.

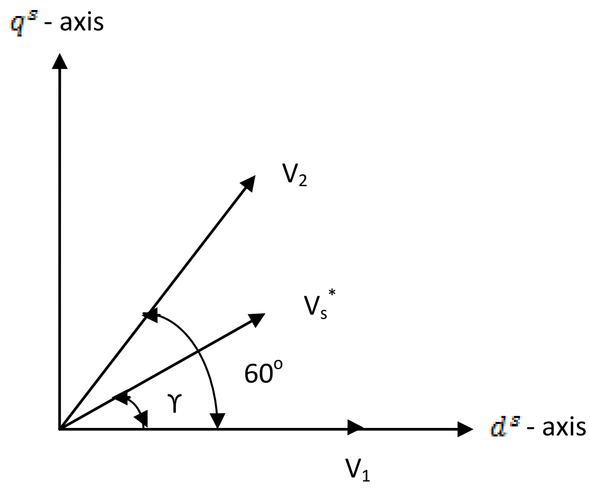

Fig.4.2 Reference vector in sector 1

The Fig 4.2 shows that in sector 1, the space voltage vector V_1 is lie along α-axis, makes an angle 60º with V_2 and making an angle γ at a particular instant with V_s^*. In order to generate the reference space vector in sector 1, the switching state vector V_1 is applied for an interval t_1 , V_2 for t_2 and the two zero vectors V_0, V_7 for interval $t_0,\ t_7$ [66] respectively. Therefore, the total sampling interval $t_s$can be written as:

$$t_s = t_1 + t_2 + t_0 + t_7 \qquad (4.3)$$

Resolving V_s^* and V_1, V_2 along the α-β axis, and by equating voltage-time integrals we get:

$$|V_s^*|\ t_s \cos\gamma = |V_1|t_1 + |V_2|t_2 \cos\frac{\pi}{3} \qquad (4.4)$$

$$|V_s^*|\ t_s \sin\gamma = |V_2|t_2 \sin\frac{\pi}{3} \qquad (4.5)$$

Dividing by V_{dc} on both sides of equation (4.4) and (4.5) and substitute a = abs ($\frac{V_s^*}{V_{dc}}$) and we get:

$$a\, t_s \sin\gamma = \frac{\sqrt{3}}{2}\, t_2$$

Or, $$t_2 = \left(\frac{2a\, t_s \sin\gamma}{\sqrt{3}}\right) \qquad (4.6)$$

and $$a\, t_s \cos\gamma = t_1 + \frac{1}{2}\, t_2 \qquad (4.7)$$

put the value of t_2 from equation (4.6) in (4.7) and multiplying both sides by $\frac{\sqrt{3}}{2}$ of resulting equation and we obtain,

$$t_1 = \frac{2\, a\, t_s}{\sqrt{3}} \sin\left(\frac{\pi}{3} - 3\right) \qquad (4.8)$$

$$t_o = t_7 = t_6 - (t_1 + t_2) \qquad (4.9)$$

If the vector is in sector 1, then the switching pattern can be determined with the help of t_0, t_1, t_2, and t_7. These four time intervals are change simultaneously when V_s* goes from one sector to another for a particular modulation index a. The six sectors with label 1, 2,….,6 are used to complete the full cycle. When Vs* is move over to sector 2, the inverter will remains in the switching state vector V_2 for the time interval t_1 and in V_3 for the time t_2. Similarly in case of sector 3: V_3 is for t_1 and V_4 is for t_2 and so on.

4.2.2 Pulse Pattern Generation

The generation of the PWM pattern means, generating the gating pulses in correct interval for the six switches of the inverter, so that the switching state vectors are active for the suitable time intervals as the reference space vector moves over a complete full cycle. In order to get the minimum switching frequency, the state of only one phase of the inverter has to be changed from $+\frac{V_{dc}}{2}$ to $-\frac{V_{dc}}{2}$ while changing the switching vectors. Fig.4.3 shows the inverter phase to dc center tap voltages and the switching frequency of the inverter is half of the sampling frequency.

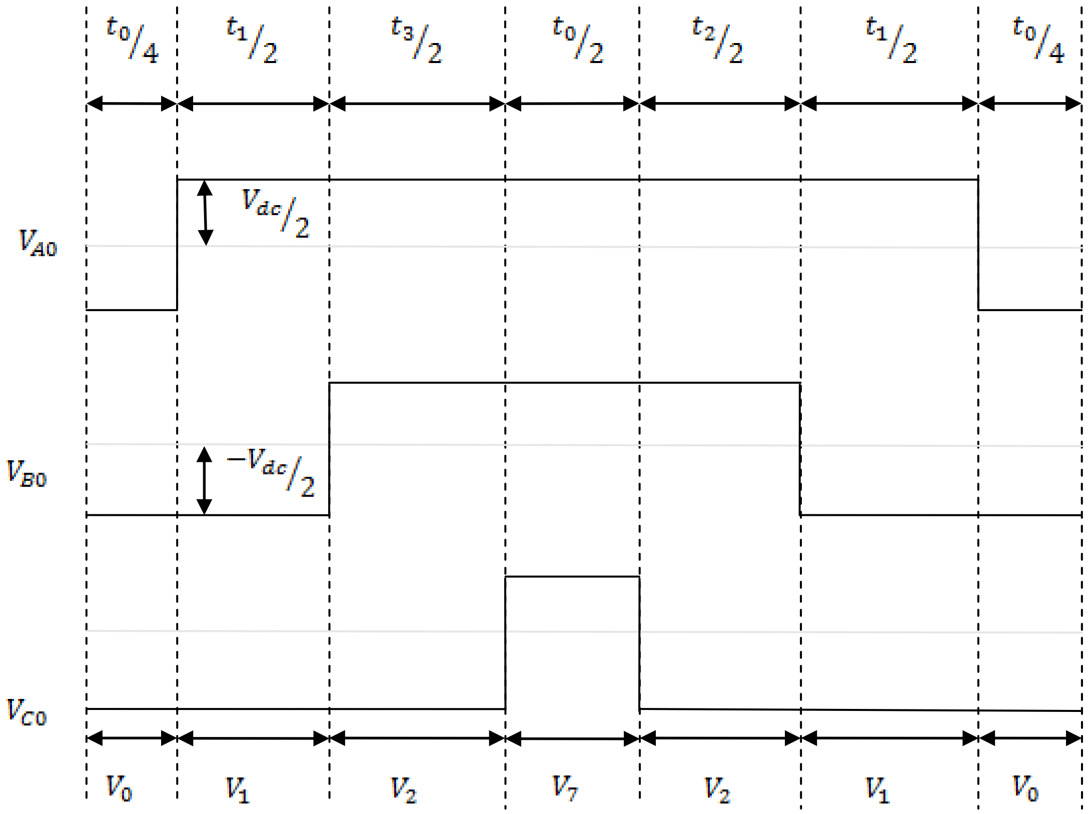

Fig.4.3 Leg voltages and space vector disposition in sector 1

The average values of the phase to center tap voltages (V_{A0}, V_{B0} and V_{C0}) can be evaluated, by taking the mean over one sampling period t_s as follows:

$$\bar{V}_{A0} = \frac{V_{dc}}{2t_s}\left(-\frac{t_0}{2} + t_1 + t_2 + \frac{t_0}{2}\right) \tag{4.10}$$

$$\bar{V}_{B0} = \frac{V_{dc}}{2t_s}\left(-\frac{t_0}{2} - t_1 + t_2 + \frac{t_0}{2}\right) \tag{4.11}$$

$$\bar{V}_{C0} = \frac{V_{dc}}{2t_s}\left(-\frac{t_0}{2} - t_1 - t_2 + \frac{t_0}{2}\right) \tag{4.12}$$

Put the value of t_1, t_2 in the above equations 4.10, 4.11 and 4.12 and we get:

$$\bar{V}_{A0} = \frac{aV_{dc}}{\sqrt{3}}\sin\left(\gamma + \frac{\pi}{3}\right) \tag{4.13}$$

$$\bar{V}_{B0} = aV_{dc}\sin\left(\gamma - \frac{\pi}{6}\right) \tag{4.14}$$

$$\bar{V}_{C0} = -\bar{V}_{A0} \tag{4.15}$$

4.3 CONCLUSION

In this chapter it has been observed that PWM generation gives better utilization of dc bus voltage for inverter. The triple harmonics which are present in the mean value of phase voltages obtained by SVPWM technique are eliminated in the line voltage and at maximum modulation index the peak value of line voltage is 15 % more than that in PWM.

CHAPTER-5

MRAS ESTIMATION TECHNIQUES

5.1 INTRODUCTION

Induction motors have been widely used in industries for variable and fixed speed applications due to advancements in power semiconductor devices, control techniques and microelectronic. These motors have advantages related to size, weight, maintenance, reliability and cost and provide fast dynamic response due to the decoupled control of flux and torque components of stator current.

Over the last two decades, IM drives have investigated sensorless control techniques and the great advantages offered by sensorless control technique was compactness and its robustness make it very much attractive for many industrial applications, specially for those drives which was operating in the hostile environments. There are many methods or ideas or schemes proposed for the sensorless IM drives, but MRAS is the most popular schemes used in the industries because of their simple implementation and less computational effort. These schemes do not usually provide a better response at low stator frequency. In order to improve the performance of MRAS-based sensorless schemes, lots of research have been devoted in this region of operation.

5.2 MODEL-BASED SENSORLESS STRATEGIES

There are many methods or schemes have been developed for the estimation of rotor speed of an IM. In these methods, mainly stator voltage and current information are used to estimate the rotor speed from the machine equations. Speed estimators can be implemented either in open loop system or in closed loop system[5, 6]. The only difference between the two schemes is the absence of a correction term in the open loop estimator [5]. Open-loop estimators do not require any form of feedback and they are directly based on the dynamic model of the machine. There are mainly two problems that can affect the estimation accuracy of these schemes especially at low speed i.e a pure integration problems and the voltage measurement noise. In addition to this the open loop estimators are very sensitive to the parameter variations and significantly affected their performance in both the transient and the steady state [5,6]. Whereas, the closed loop estimators, are usually referred to as an observers [5], an error signal between the measured quantities and the estimated quantities is used to adjust their response [4, 5] and due to this there is increase in the dynamics performance and robustness [6]. On the basis of plant representation, the observers are classified as deterministic and stochastic. The most commonly used non linear estimators are Luenberger and Kalman, the extended Luenberger observer (ELO) are applied to the nonlinear, time-varying deterministic system, whereas extended Kalman filter (EKF) is applied to the nonlinear, time-varying stochastic systems [5]. In both the observers ELO and EKF, the rotor speed acts as a state variable, whereas in case of full-order adaptive state observer the speed is considered as a parameter [5]. The main advantage of the ELO and EKF is that they can combine both the parameter and the state estimation. The EKF schemes are applied to the rotor speed estimation of sensorless IM drives. Whereas ELO is applied for the joint estimation of rotor flux and rotor speed estimation. Due to simplicity and effectiveness, MRAS schemes are applied for sensorless control applications.

5.3 MRAS FOR SENSORLESS CONTROL

Adaptive control is defined as a control system that can change the output of the system in response to changes in the dynamics process and the character of the disturbances. It can be realized by different strategies such as: gain scheduling, model reference adaptive control, self-tuning regulators and dual control.

Various control techniques are available for the estimation of speed for IM drive. These are classified as following:

- Rotor flux based
- Frequency signal injection method
- Model Reference Adaptive System (MRAS)
- Observer based
- Artificial Intelligence (AI) based

The best scheme among all is the MRAS are the best one because of its simplicity, less computational time, and has a good stability. There are different types of MRAS scheme are available in the literature, which are given as follows.

- Flux based method
- Back EMF based
- Reactive power based

The flux based MRAC estimate the rotor speed in all the four quadrants operations but has some problems related to integrator at a low speed and zero speed. Back emf based MRAS are also less efficient at low speed because at low speed back-emf is very low and the last one, the reactive power based MRAS has no problem related to integration and using instantaneous reactive power in reference model and steady state field oriented power in the adjustable model. Therefore this method is suitable for low speed region and even at zero speed. This technique does not depend on the stator resistance and it is unstable in regenerative mode of operation.

The MRAC which uses cross product of voltage and current called as X-MRAC in which instantaneous value of voltage and current are used in the reference model and steady state flux oriented value are used in the adjustable model. This technique is stable in all the four quadrants operations and at low speed and zero speed and is discussed below.

5.3.1 Speed Estimation Based on X-MRAC

The cross product of voltage and current in synchronously rotating reference frame are used for the construction of MRAC. In which the instantaneous value of voltage and current i.e. $\vec{v}$ x $\vec{i}$ is used in reference model, whereas steady - state flux-oriented value of voltage and current are used in adjustable model. The value of $\vec{v}$ x $\vec{i}$ is adjusted such that the proposed system is stable in all the four quadrants of operation.

For the construction of X-MRAC for IM, we consider the stator voltage in the synchronously rotating reference frame which can be expressed as follows:

$$v_{qs} = R_s i_{qs} + \omega_e \sigma L_s i_{ds} + p\sigma L_s i_{qs} + \frac{L_m}{L_r}\left(\omega_e \varphi_{dr} + p\varphi_{qr}\right) \quad (5.1)$$

$$v_{ds} = R_s i_{ds} - \omega_e \sigma L_s i_{qs} + p\sigma L_s i_{ds} - \frac{L_m}{L_r}\left(\omega_e \varphi_{qr} - p\varphi_{dr}\right) \quad (5.2)$$

Where, p is the derivative operator. The instantaneous value of the fictitious quantity X= ***v*** x **i** is defined as:

$$X_1 = v_{qs}i_{ds} + v_{ds}i_{qs} \tag{5.3}$$

Substituting eqns (5.1) and (5.2) in (5.3) yields:

$$X_2 = \left\{R_s i_{qs} + \omega_e \sigma L_s i_{ds} + p\sigma L_s i_{qs} + \frac{L_m}{L_r}(\omega_e \varphi_{dr} + p\varphi_{qr})\right\} i_{ds} + \left\{R_s i_{ds} - \omega_e \sigma L_s i_{qs} + p\sigma L_s i_{ds} - \frac{L_m}{L_r}(\omega_e \varphi_{qr} - p\varphi_{dr})\right\} i_{qs} \tag{5.4}$$

At steady state,

$$X_3 = \left\{R_s i_{qs} + \omega_e \sigma L_s i_{ds} + \frac{L_m}{L_r}(\omega_e \varphi_{dr} + p\varphi_{qr})\right\} i_{ds} + \left\{R_s i_{ds} - \omega_e \sigma L_s i_{qs} - \frac{L_m}{L_r}(\omega_e \varphi_{qr} - p\varphi_{dr})\right\} i_{qs}$$

(5.5)

However, $\varphi_{dr} = i_{ds}L_m$ in rotor flux oriented drive hence

$$X_4 = \omega_e\left[L_s i_{ds}{}^2 - \sigma L_s i_{qs}{}^2\right] + 2R_s i_{ds} i_{qs} \tag{5.6}$$

The expression of X_1 is independent of rotor speed. Hence, it is selected for the reference model. X_2, X_3 or X_4 can be chosen as the adjustable model since they are dependent on the rotor speed (ω_r).However, X_4 is selected in the adjustable model, as it does not require any flux estimation and any derivative operations.

The block diagram of X-MRAC for speed estimation is shown in the Fig. 5.1, where the cross product of voltage and current are selected as a functional candidate of the MRAC. This cross product is denoted by “X” and $\vec{v}$ x $\vec{i}$ is neither reactive power nor active power. Here X_1 denotes the instantaneous value of X and X_4 denotes the steady state flux oriented value of X. The error of the two signals (i.e. ε = X_1- X_4) is given to the adaptation mechanism, which results in the estimated rotor speed ω_{rest}. This estimated speed is fed back to adaptive model so that error converges to zero. The X-MRAC for the estimation of speed as shown in Figure 5.1.

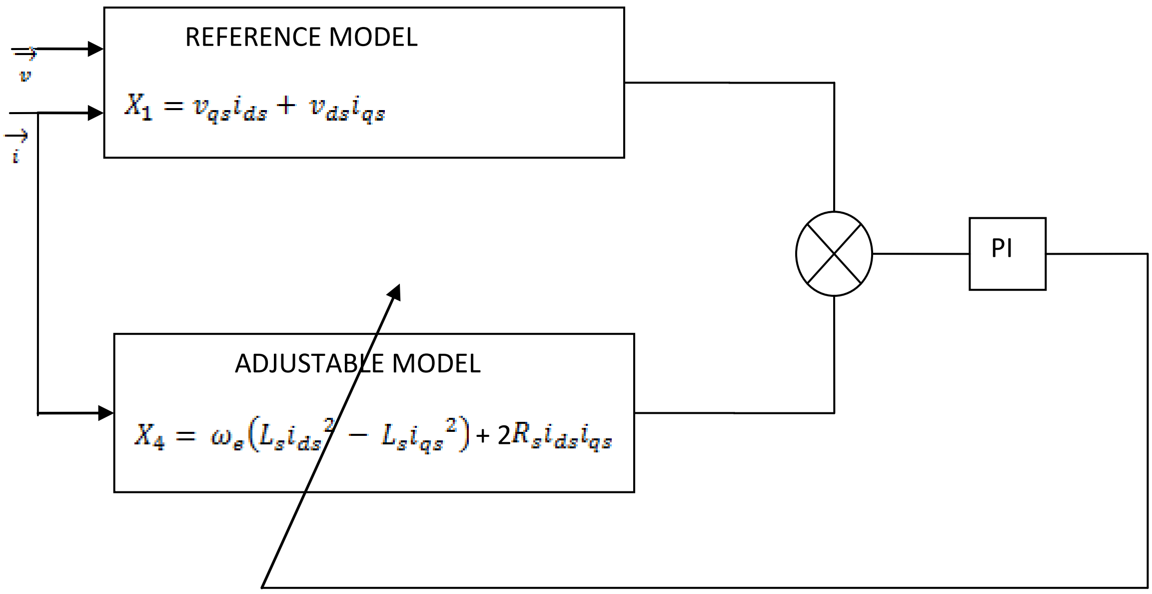

Fig.5.1 MRAC based speed estimation technique

But the adjustable model of this MRAS is dependent on stator resistance which may changes during low speed operation. So the stator resistance has to be updated if there is any stator resistance variation.

5.4 STATOR RESISTANCE ESTIMATION TECHNIQUE

For the estimation of stator resistance, the same technique has been used as above for the speed estimation i.e. X-MRAC. In case of stator resistance estimation, the induction motor stator voltages in the synchronously rotating reference frame are given by the equations (5.1) and (5.2) and for a field oriented drive, the expression of voltages at steady state (i.e., derivative terms, p = 0) becomes:

$$v_{qs} = R_s i_{qs} + \left(\frac{L_m^2}{L_r} + \sigma L_s\right)\omega_e i_{ds} \tag{5.7}$$

$$v_{ds} = R_s i_{ds} - \omega_e \sigma L_s i_{qs} \tag{5.8}$$

Using equation (5.7) and (5.8), stator resistance is derived as:

$$R_s = \frac{v_{ds} i_{ds} + \sigma v_{qs} i_{qs}}{\sigma i_{qs}^2 + i_{ds}^2} \tag{5.9}$$

The expression for R_s is independent of speed, and is estimated using voltage and current in synchronously rotating reference frame as shown in Fig 5.2.

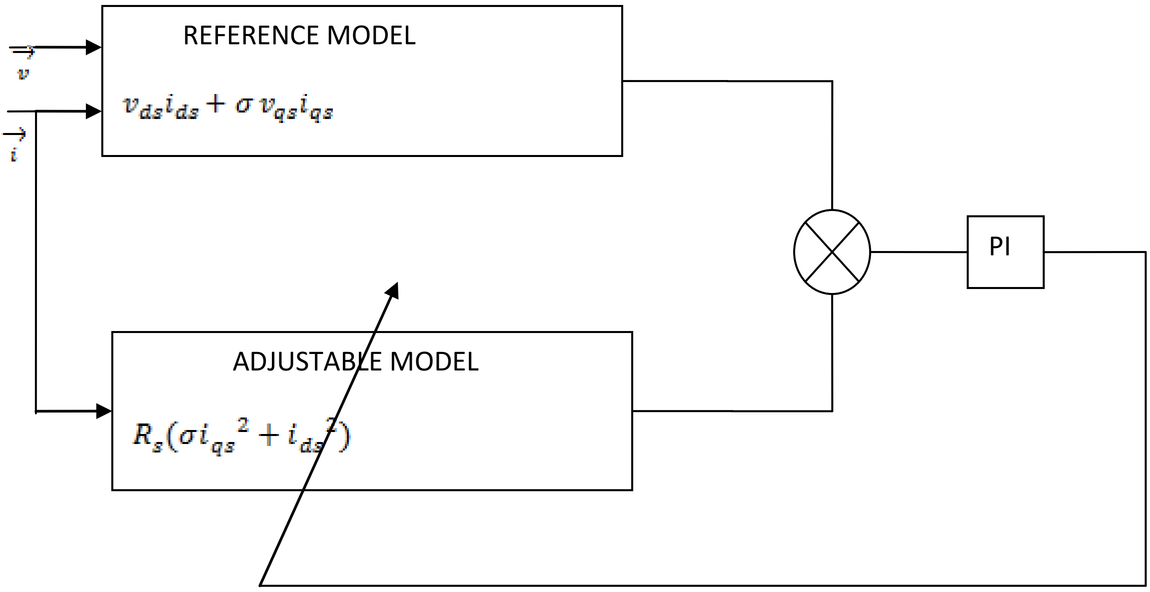

Fig.5.2. MRAC based stator resistance estimation technique

In the above Fig. 5.2 the stator currents are sensed and then transformed from abc to synchronously rotating frame quantities i_{ds} and i_{qs}. Stator voltages are also sensed and transformed to synchronously rotating frame quantities (d-q) v_{ds} and v_{qs}. Using these voltages and currents in synchronously rotating reference frame, the rotor speed and stator resistance, R_s is estimated.

5.5 CONCLUSION

This chapter has provided a detailed review of different model based techniques applied to speed sensorless IM drives with most emphasis is given to the MRAS. Model Referencing Adaptive Controller (MRAC) based on speed and stator resistance estimation of vector controlled induction motor drive is explained. Both the MRACs required voltages and currents in synchronously rotating reference frame for estimation of rotor speed and stator resistance. The speed estimation algorithm (i.e. speed estimating MRAS) depends on stator resistance and R_s estimation algorithm is independent of speed. The proposed method is simulated in MATLAB/SIMULINK and simulation results are obtained.

CHAPTER-6

SIMULATION MODEL RESULTS AND DISCUSSION

6.1 INTRODUCTION

Induction motors have been the area of research due to its ruggedness and longevity. There is an implementation of new control techniques, due to advancement in the power electronics. Numerical simulation tools are an important tool to verify the operation of new controllers. In this study, MATLAB/ Simulink simulation software, a mathematical tool developed by the Mathworks, has been used to verify the results. Vector Control of IM using PI controller and MRAS technique has been simulated and the results are presented.

6.2. Block diagram overview of vector controlled induction motor

The complete block diagram of three phase induction motor is shown in the Figure 6.1 which is used for mathematical modeling and simulation studies estimation. It can be seen that the block diagram consist of PI controllers , d-q to abc transformation blocks, the IM models and various controllers.To validate the developed X-MRAS rotor speed and stator resistance estimator on a sensor-less vector control, simulation studies are carried out of a 1.5 HP induction motor drive using Matlab/Simulink with parameters are given in Table 6.1.The performance of the induction motor is studied under various operating conditions.

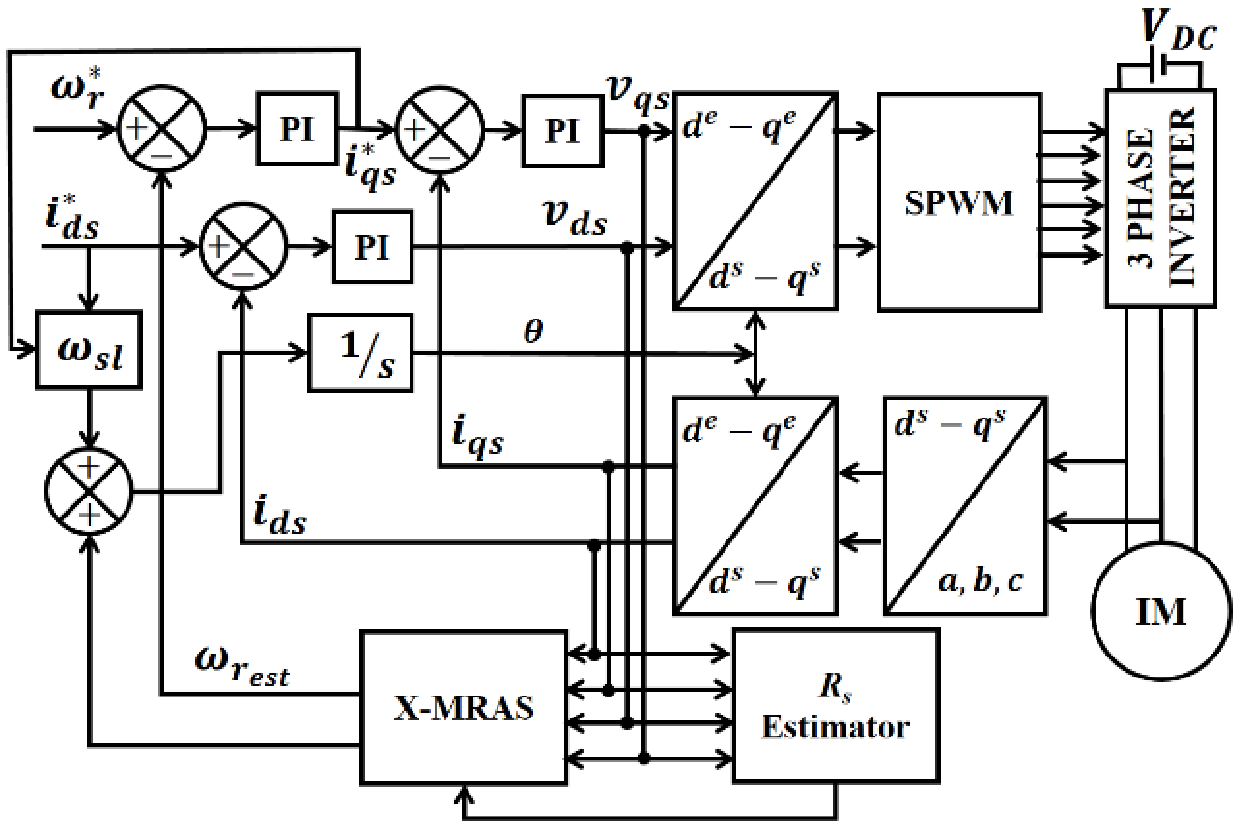

Fig.6.1 Block diagram of vector controlled induction motor with MRAS based stator resistance estimation

6.3. RESULTS

To validate the developed X-MRAS stator resistance estimator on a sensor-less vector control, simulation studies are carried out on a 1.5HP IM using Matlab/ Simulink with parameters given in Table 6.1.

TABLE 6.1 – PARAMETERS OF 1.5HP, 415V, 1430 RPM IM

Parameter	Value
Pair of Pole	2
L_s , L_r , L_m	0.5192H , 0.5192H , 0.4893H
R_s , R_r	6.03Ω , 6.085Ω
Moment of J	0.01178Kg-m^2

The performance of the IM drive is studied under various operating conditions. The developed algorithm is tested for step change in speed, ramp variation in speed, low-speed operation etc. The results obtained as given at Figs. 6.2 to 6.7 are discussed in the succeeding paragraphs.

6.3.1 Performance of IM for Step Speed change under no – load condition

The no-load step speed response of the IM for four quadrants of operation is shown in Fig. 6.2(a). The speed reference is set to zero from t=0 to t=5 secs. At t=5secs a step change of 20 rad/s is given for the next 5 secs. At t=10 secs, a speed reversal from 20 rad/sec to -20 rad/sec is applied for 5 seconds. This cycle is repeated over a period of 30 seconds. The estimated speed tracks the actual speed very closely. It is also observed that there is no effect on the rotor flux during the aforesaid operation, as depicted in Fig.6.2(b) and Fig. 6.2 (c) shows three phase current and zoom view of Fig. 6.2(c) as shown in Fig. 6.2 (d).

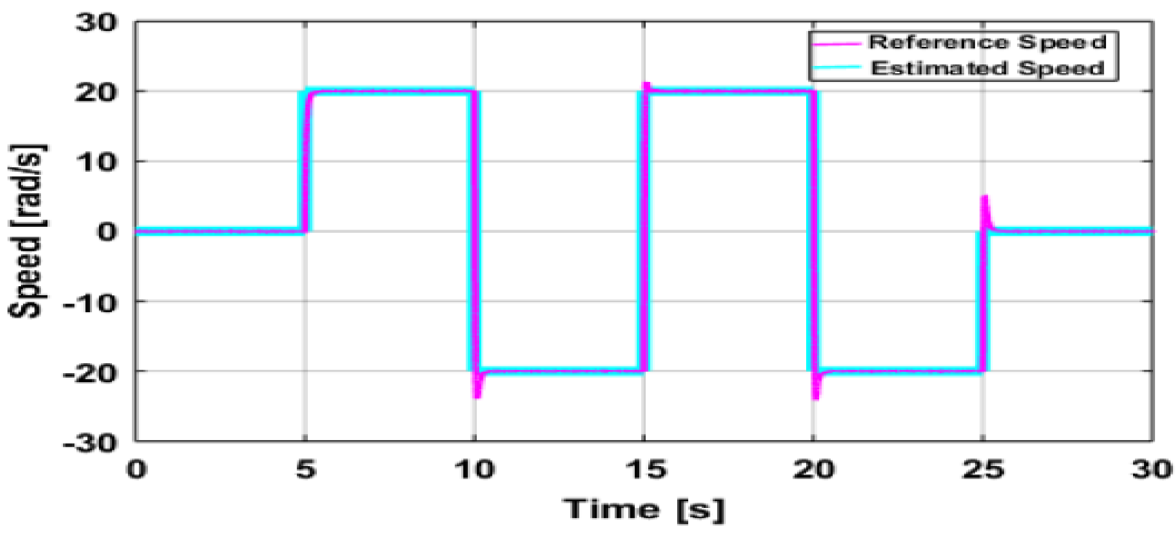

Fig. 6.2 (a) No-load speed response of IM

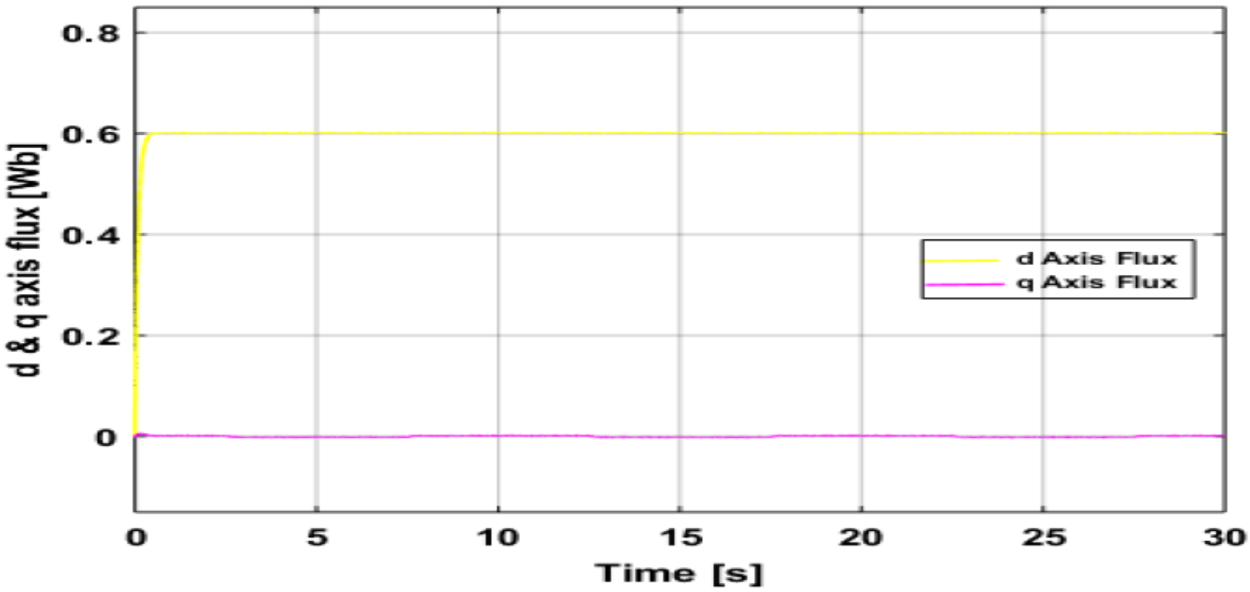

Fig.6.2 (b) d and q-axes Rotor flux response for no-load operation of IM

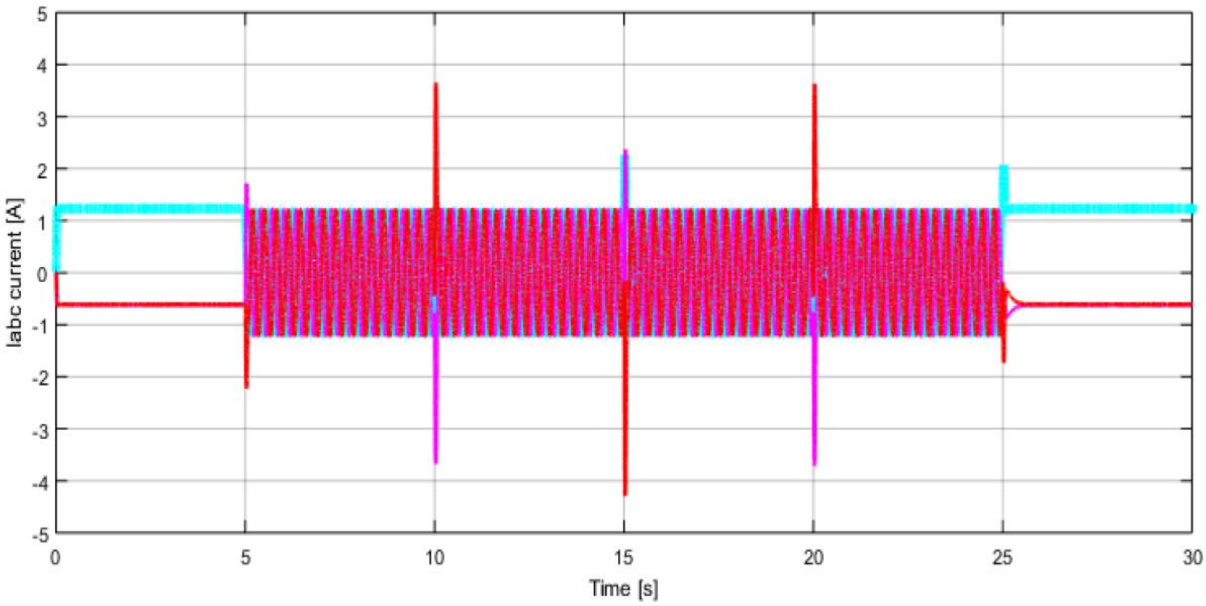

Fig.6.2 (c) Iabc response for no-load operation of IM

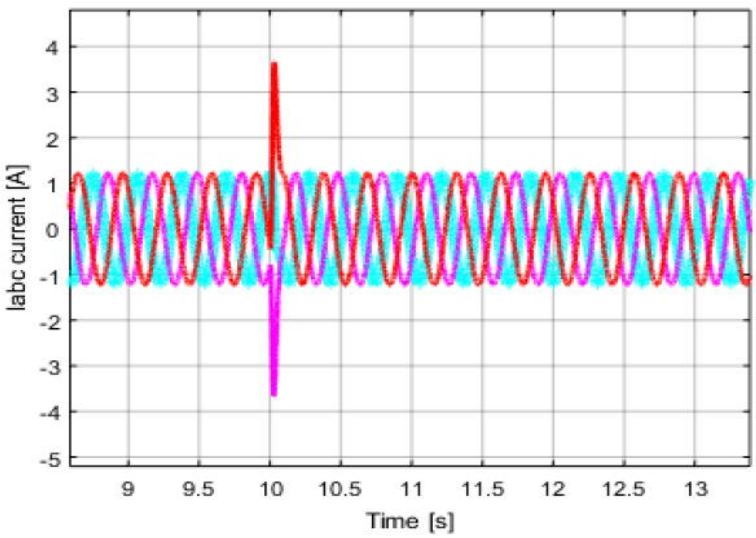

Fig.6.2 (d) Iabc response for no-load operation of IM

6.3.2 Performance of IM for Step Speed Change Under Loaded Condition

The speed response of the IM at a load of 5Nm for four quadrants of operation is shown in Fig. 6.3 (a). After 5 secs of operation of IM at zero speed, a step change in speed of 15rad/sec is applied for 10 secs, followed by a speed reversal at t=15secs. The IM is operated at -15 rad/sec for the next 10 secs and this cycle is repeated. It is observed that the estimated speed tracks the reference speed and there is no torque variation corresponding to change in speed as shown in Fig. 6.3(b) and Iabc current in Fig. 6.3 (c) and zoom view of Fig. 6.3(c) as shown in Fig. 6.3(d).

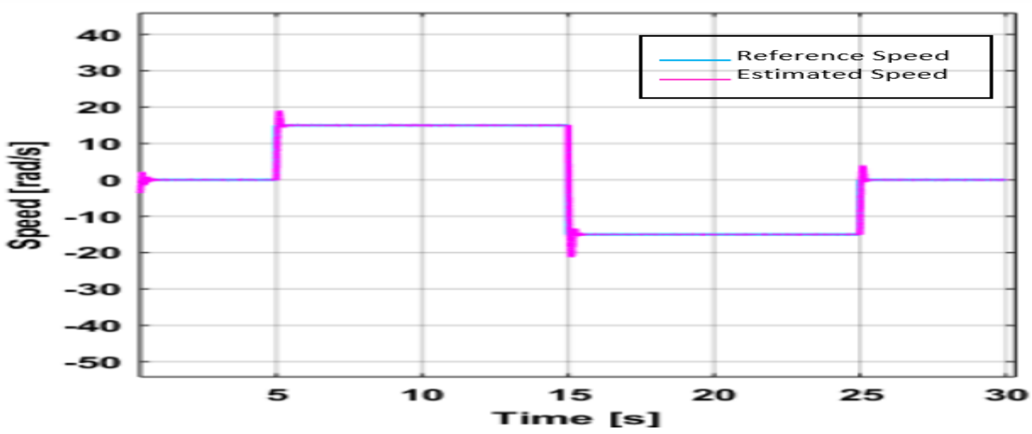

Fig. 6.3 (a) Speed response for operation of IM under loaded condition

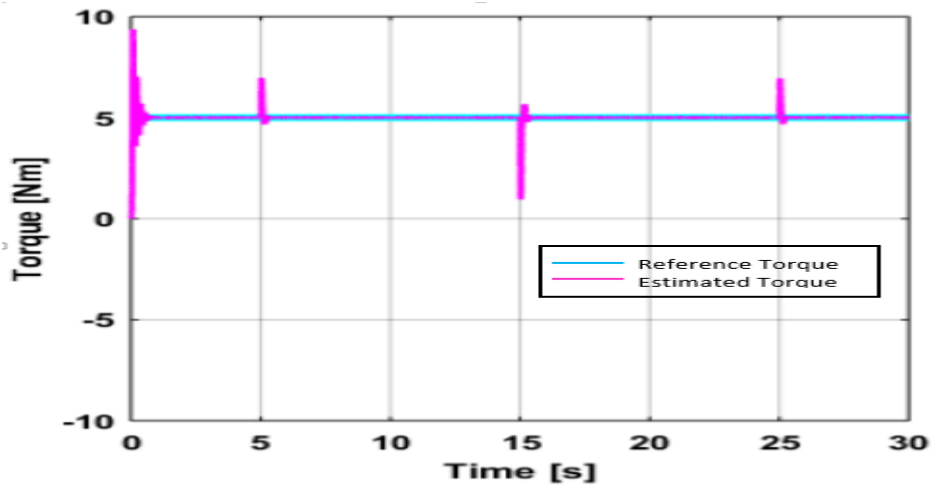

Fig. 6.3(b) Torque response for operation of IM under loaded conditions

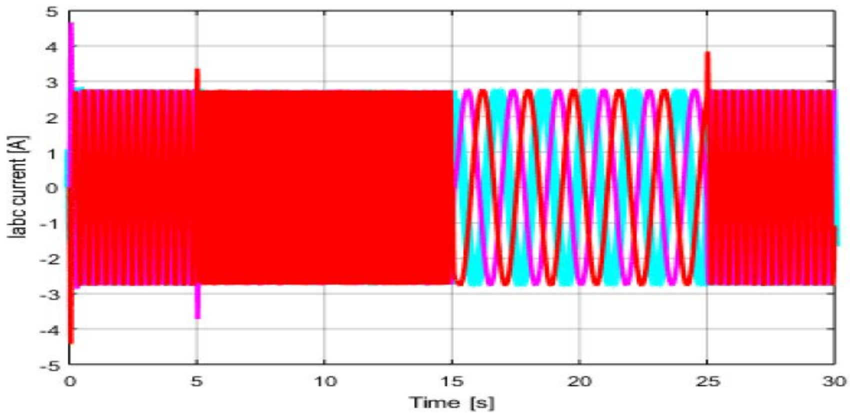

Fig.6.3 (c) Iabc response for load torque 5 Nm

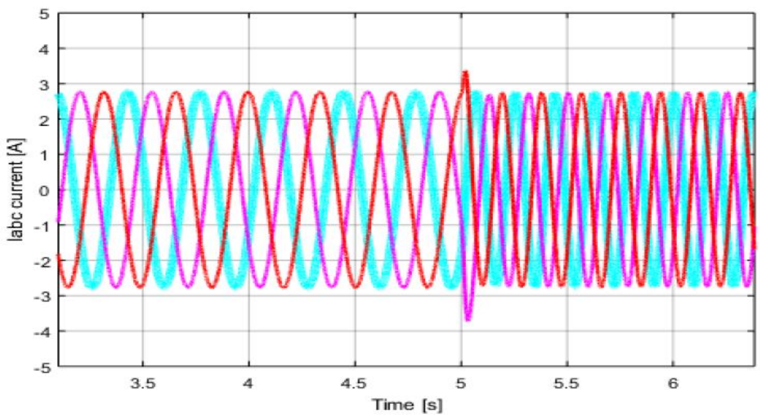

Fig.6.3 (d) Iabc response for load torque 5 Nm

6.3.3 RAMP SPEED RESPONSE OF IM

The low speed, four quadrant operation of the IM is validated by the application of a ramp signal as shown in Fig. 6.4(a). The estimated speed tracks the actual motor speed, which matches the applied input ramp signal. In the above operations, the flux orientation is maintained as shown in Fig. 6.4(b). Stable operation of the IM in forward and reverse-motoring modes is thus validated.

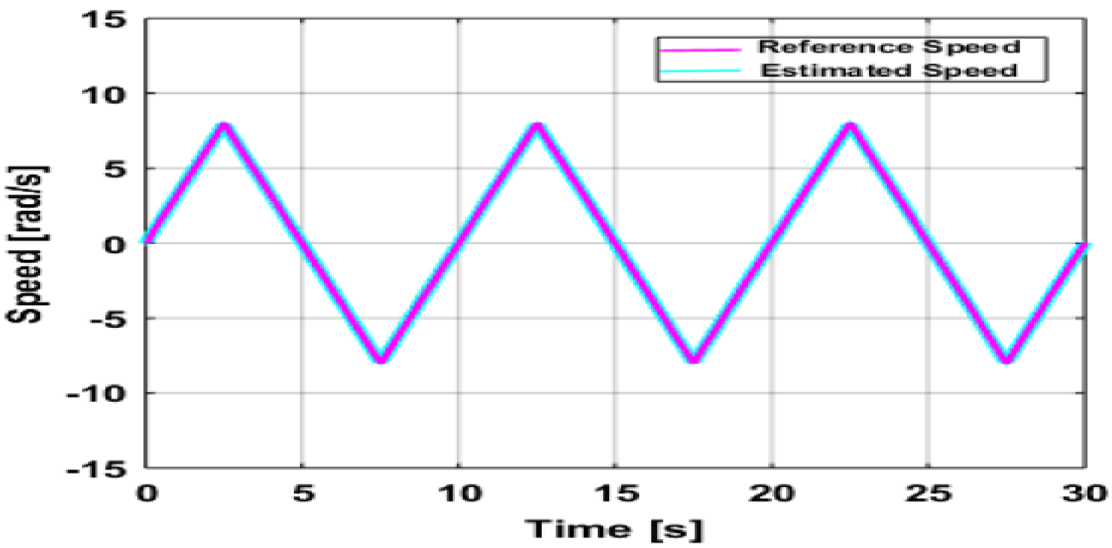

Fig. 6.4 (a) Speed response of IM for ramp signal

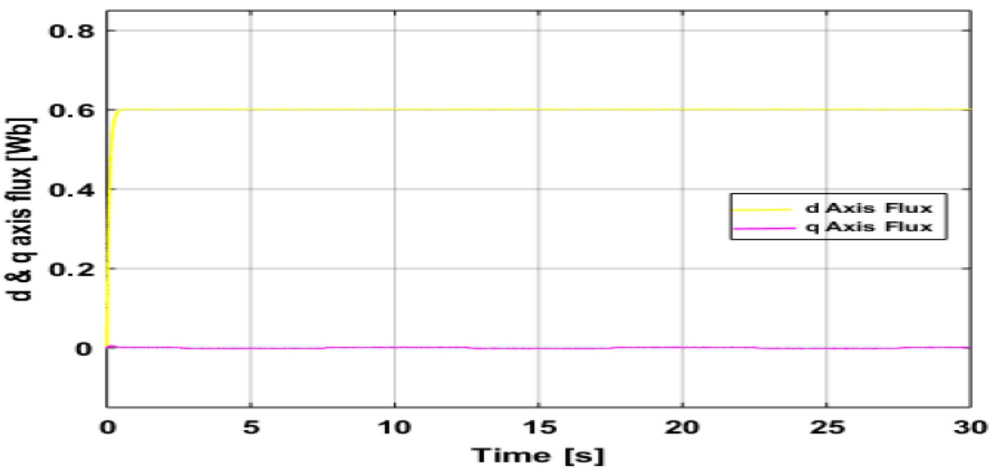

Fig. 6.4 (b) d and q-axes Rotor flux response for ramp signal

6.3.4 LOW SPEED OPERATION OF IM UNDER LOADED CONDITION

The IM drive is operated at a low speed of 5 rad/s with a load torque of 3Nm with the developed model. The corresponding speed response is shown in Fig.6.5 (a). The flux orientation is maintained, as shown in Fig.6.5 (b) and the torque response and current response is given in Fig.6.5(c) and Fig. 6.5(d). The zoom view of Fig. 6.5(d) is shown in Fig. 6.5(e). Stable operation of the IM in forward motoring mode under low speed operation is thus validated.

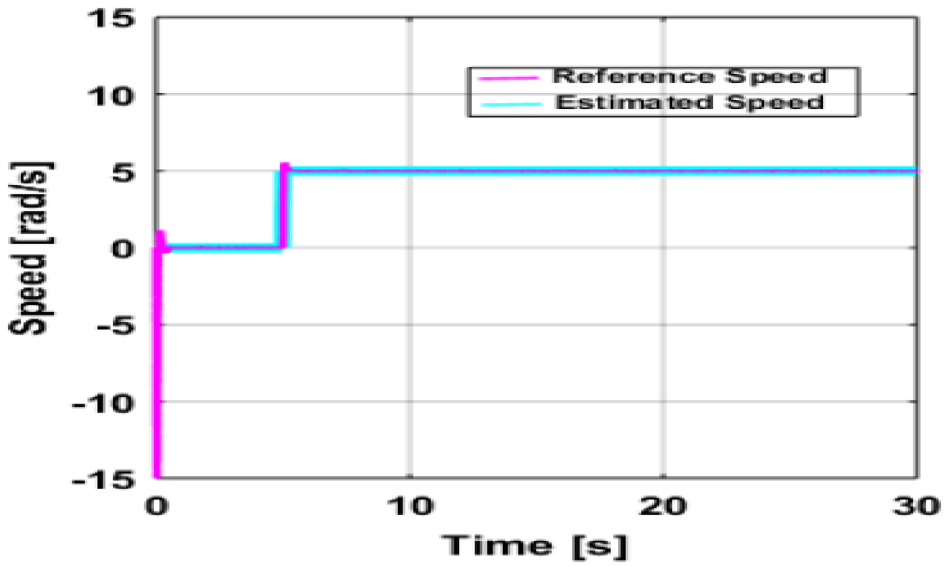

Fig. 6.5 (a) Speed response for Low Speed Operation of IM under loaded condition.

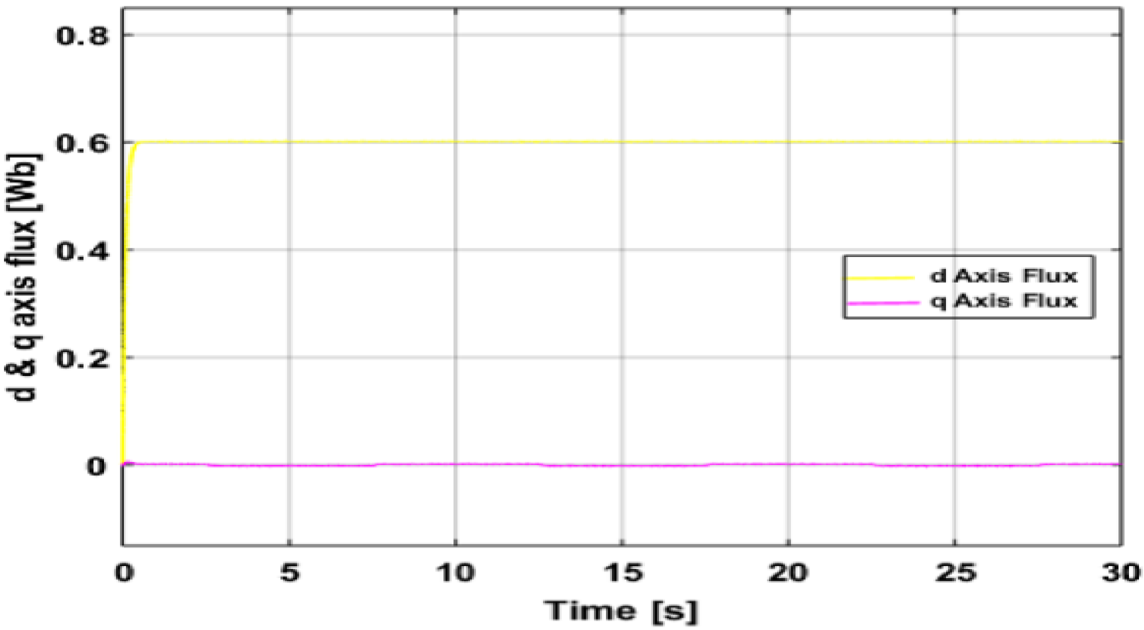

Fig. 6.5 (b) d and q-axes Rotor flux response for Low Speed Operation of IM under loaded condition

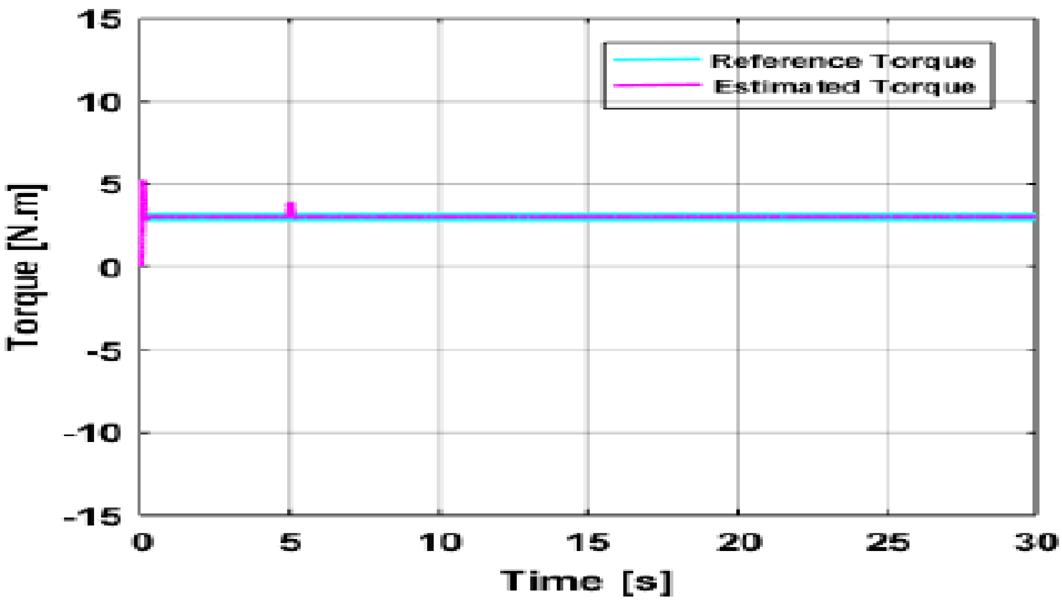

Fig. 6.5 (c) Torque response for Low Speed Operation of IM under loaded condition.

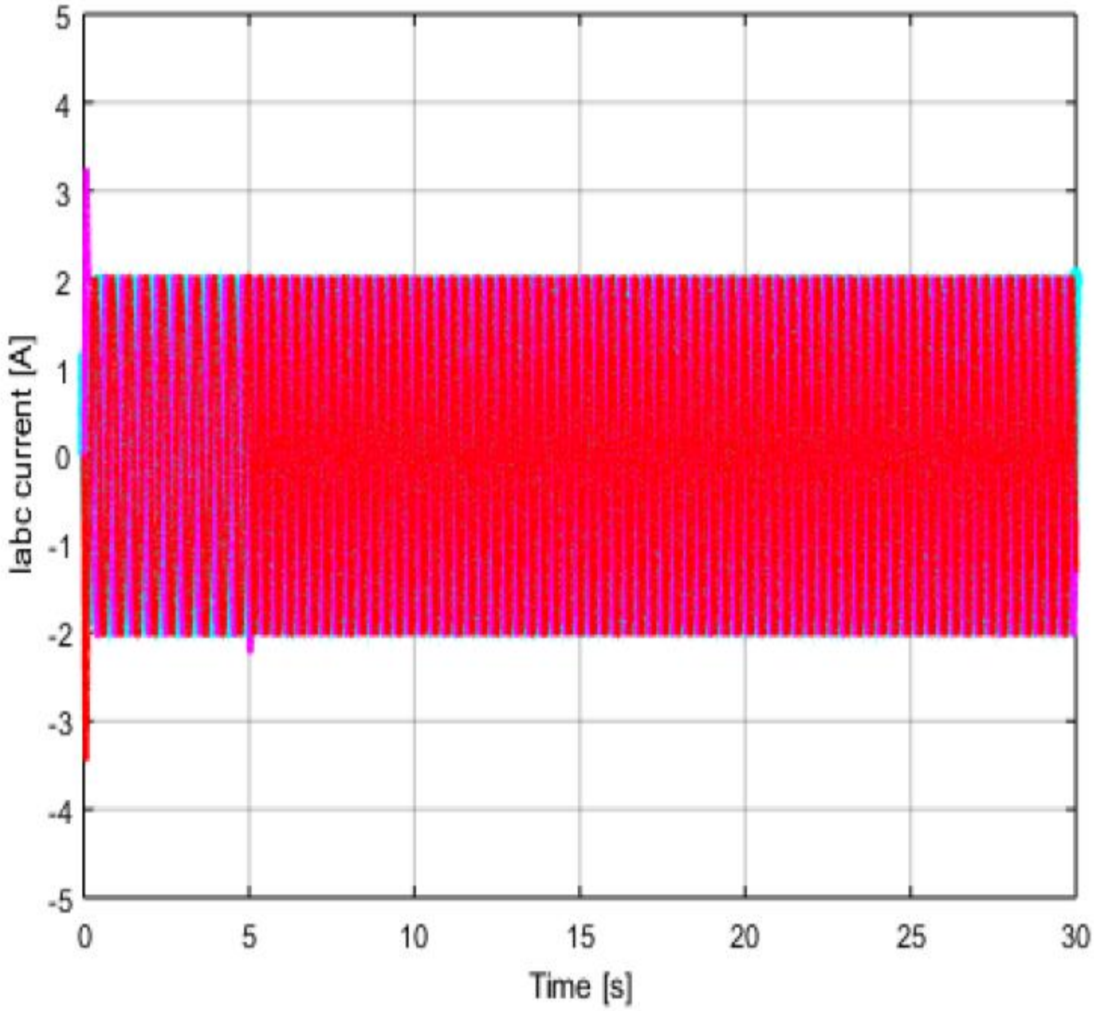

Fig. 6.5 (d) Iabc current response for Low Speed Operation of IM

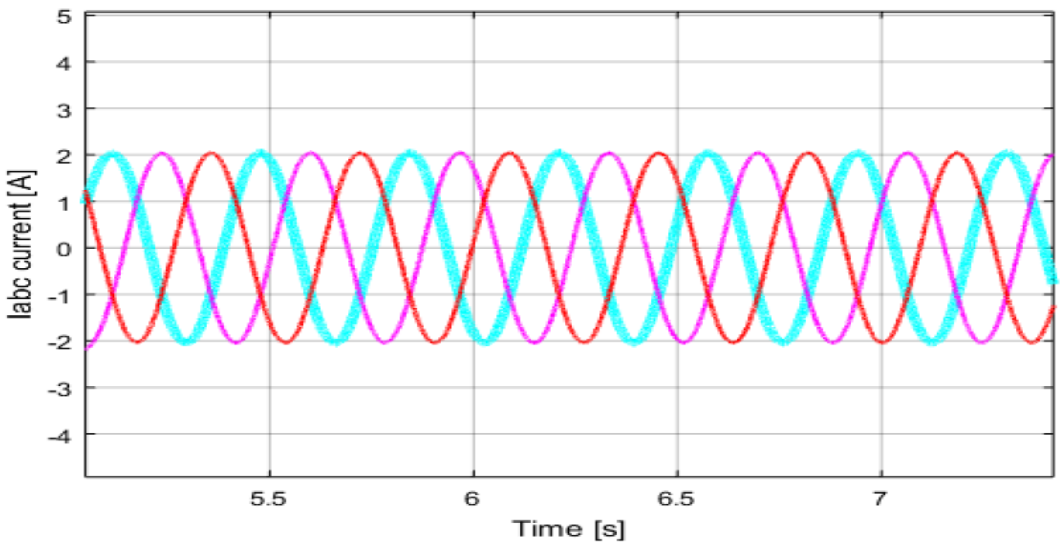

Fig. 6.5 (e) Iabc current response for Low Speed Operation of IM

6.3.5 HIGH SPEED PERFORMANCE OF IM UNDER LOAD AND R_s VARIATION

The model is tested for high speed operation considering load and resistance variation for motoring and regenerating modes of operation. The developed algorithm is tested for high speed operation considering variation in R_s under variable torque condition. The speed, torque, and resistance variation of the IM and Iabc current response are shown in Figs. 6.6(a), 6.6(b), 6.6(c) and 6.6(d) respectively. The zoom view of Fig. 6.6(d) is shown in Fig. 6.6(e).

At t=5 secs a step change of 50 rad/sec is applied to the IM at rest under no-load condition. At t=7.5 secs a load of 3 Nm is applied to the IM followed by an increase in speed to 100rad/sec at t=15 secs. The motoring mode of operation of the IM is validated along with a step change in stator resistance to double it's value from t=5 secs to t=15 secs. During this motoring operation, the IM is subjected to a load change from 3Nm to 2.5 Nm at t=18 sec. At t=25 secs a step change of speed from 100 rad/sec to rest is applied to the IM. It is observed that the rotor speed closely tracks the reference speed.

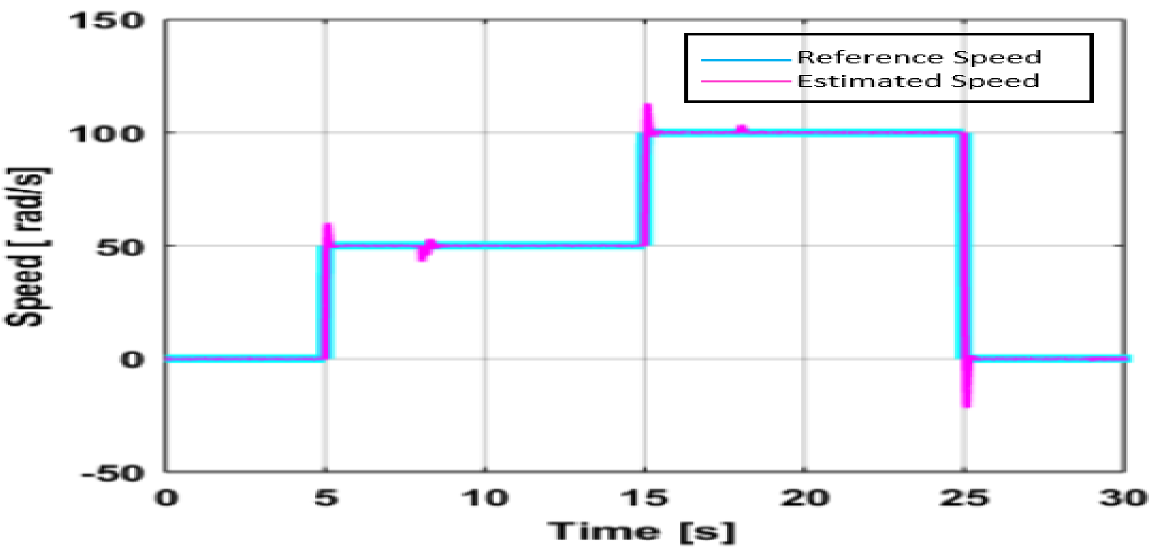

Fig. 6.6 (a) Speed response of IM for High Speed Operation

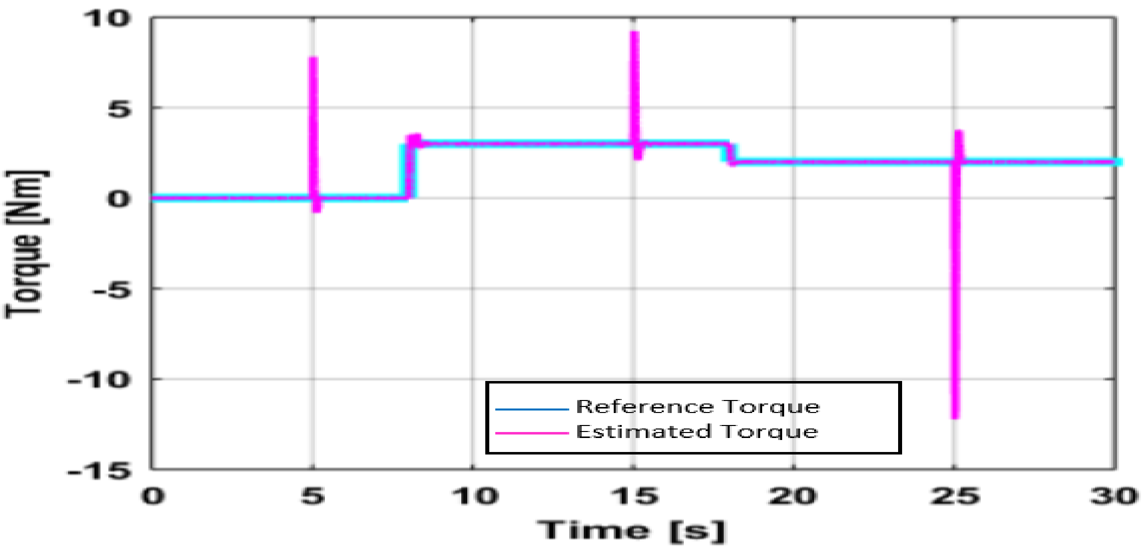

Fig. 6.6 (b) Torque response of IM for High Speed Operation

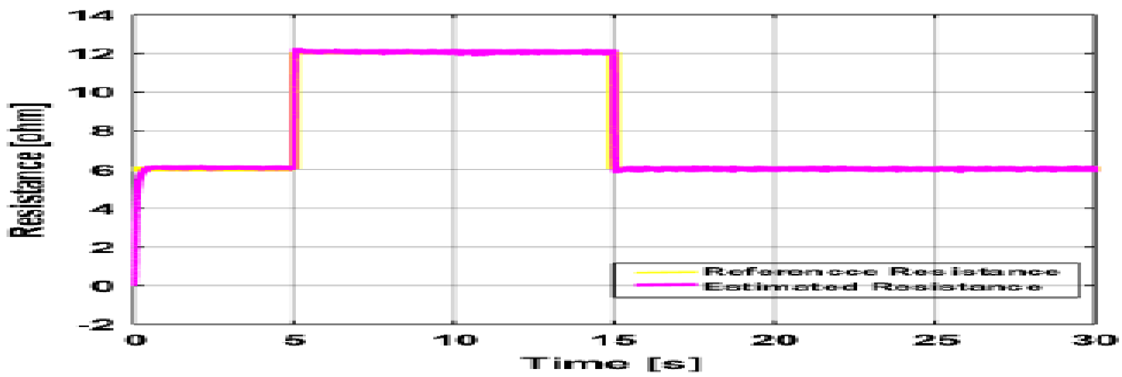

Fig. 6.6 (c) Variation of R_s in IM for High Speed Operation

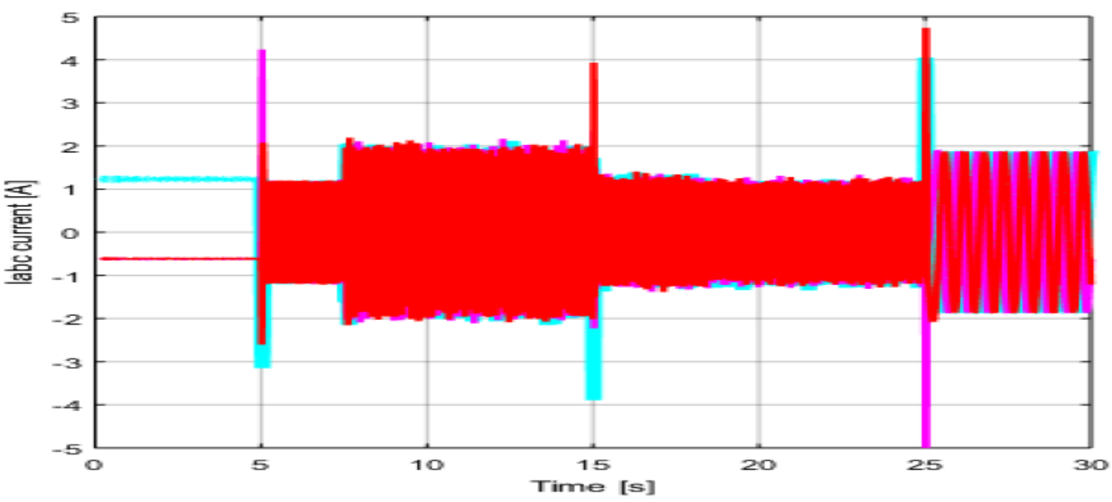

Fig. 6.6 (d) Iabc response of IM for High Speed Operation

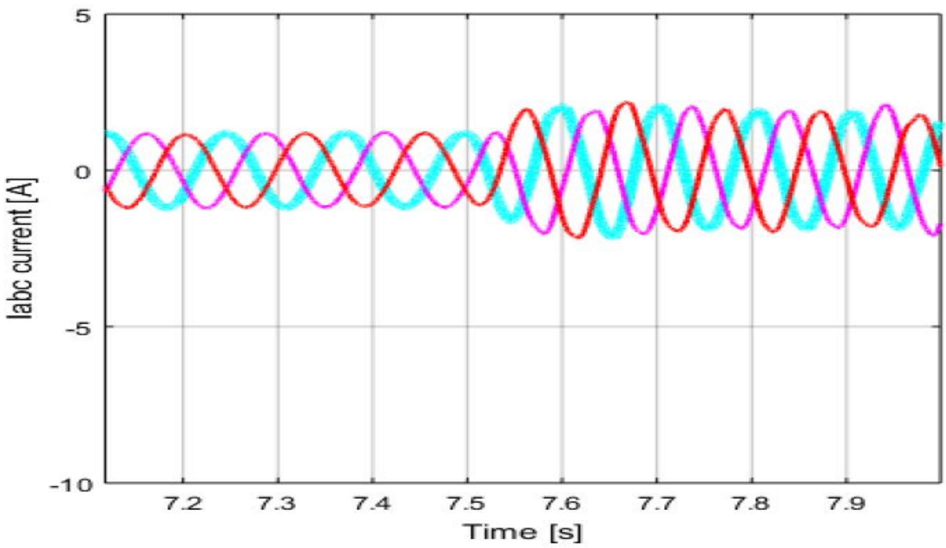

Fig. 6.6 (e) Iabc response of IM for High Speed Operation

6.3.6 Low Speed Performance of IM under Load and Rs Variation

The model is tested for low speed operation at 4 rad/sec, as shown in Fig. 6.7(a), under variation of load torque in the form of step input from 2 Nm to 4 Nm, as shown in Fig. 6.7(b). Rs is varied in the form of a ramp from its initial value of $6.03\ \Omega$ at $t = 10$ sec, to twice its value at $t = 23$ sec, as shown in Fig. 6.7(c). It is observed that the rotor speed closely tracks the reference speed for a ramp change in Rs and a step change in load torque for low speed operation of IM. The Iabc current is shown in Fig. 6.7(d).

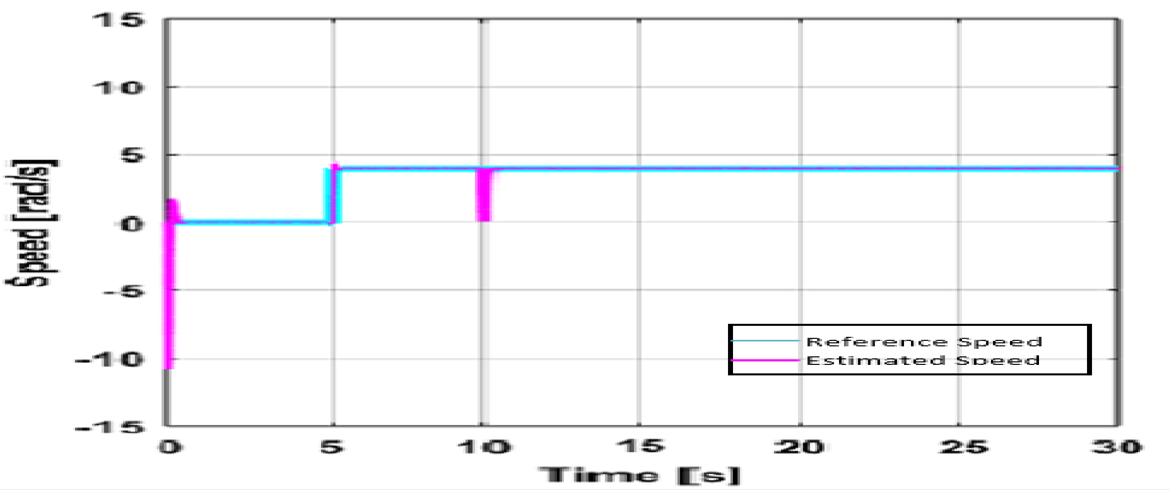

Fig. 6.7 (a) Speed response of IM for Low Speed Operation

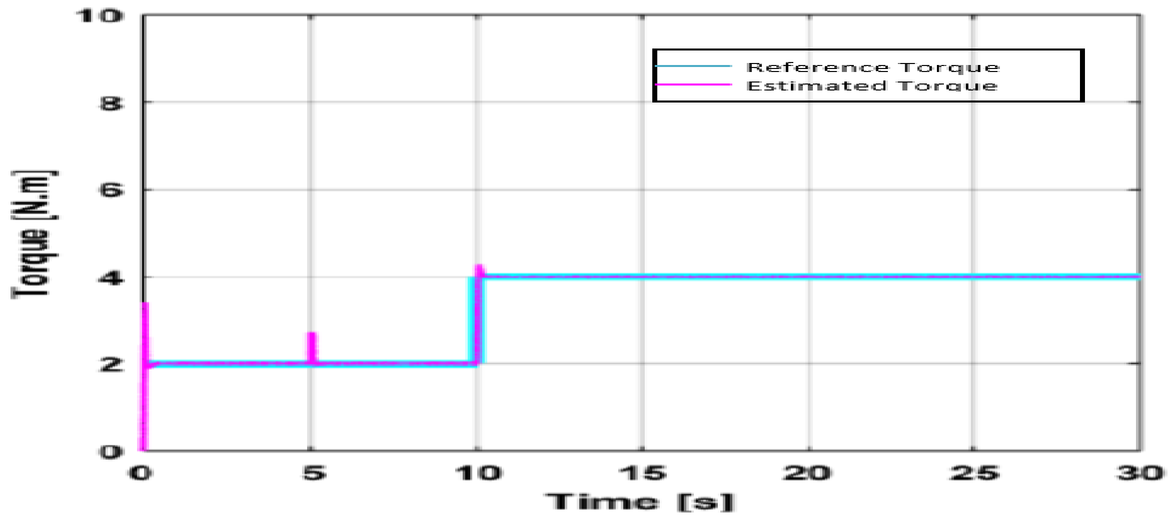

Fig. 6.7 (b) Torque response of IM for Low Speed Operation

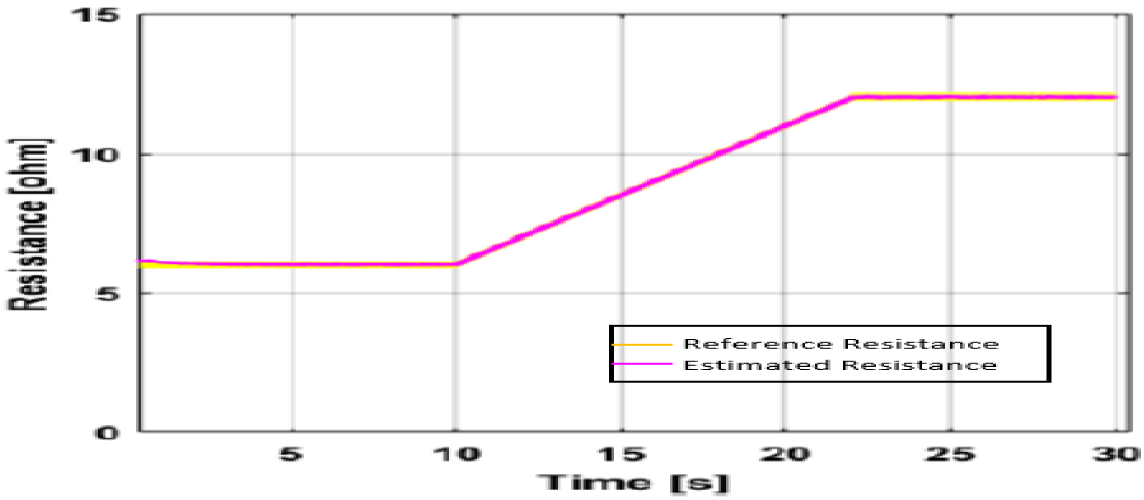

Fig. 6.7 (c) Variation of R_s in IM for Low Speed Operation

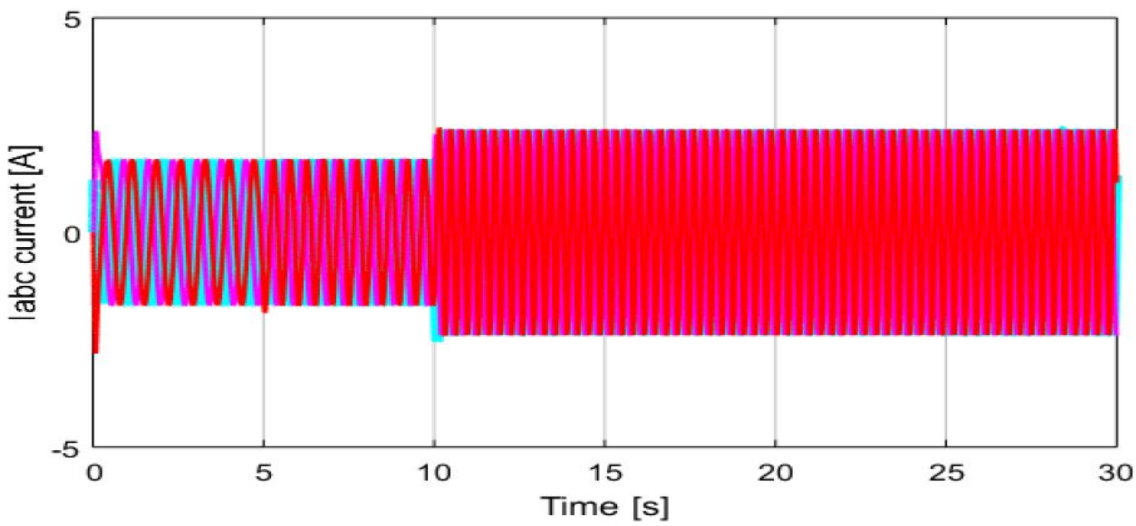

Fig. 6.7 (d) Iabc current response of IM for Low Speed Operation

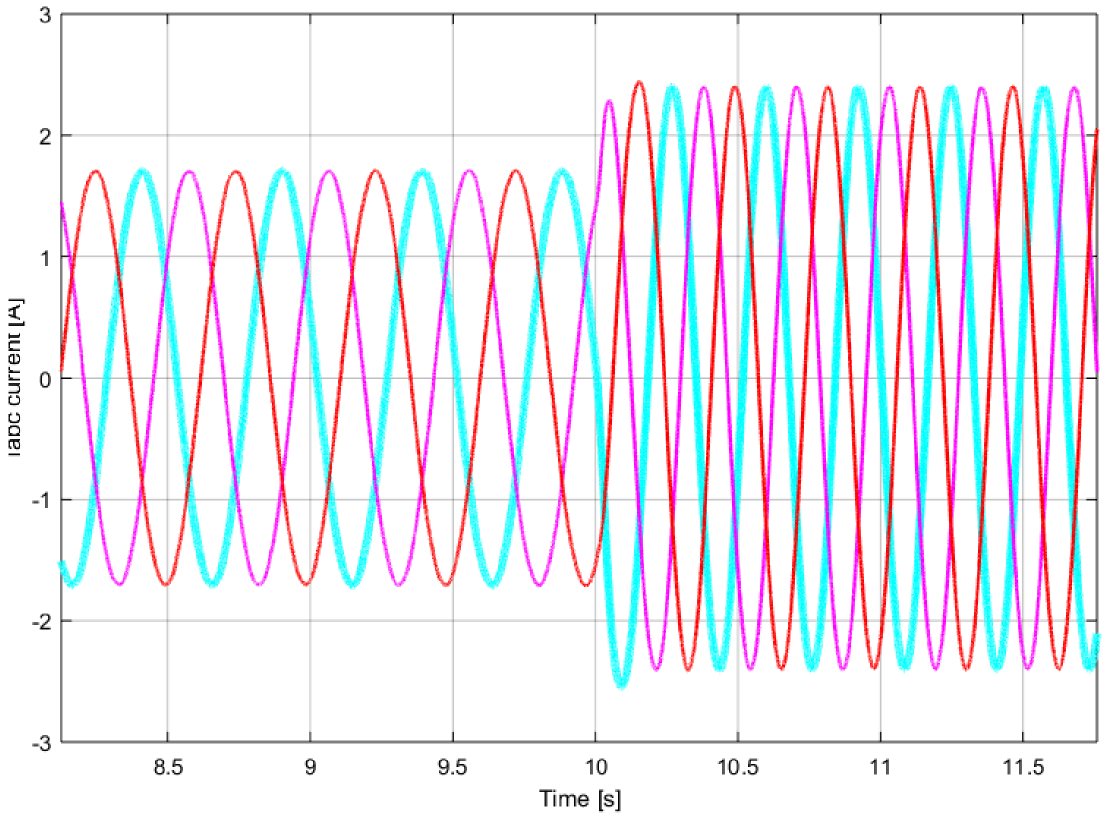

Fig. 6.7 (e) Iabc current response of IM for Low Speed Operation

6.4 CONCLUSION

The speed and stator resistance estimator is capable of tracking the stator resistance variations very well. The transient performance of the proposed sensorless drive is presented, when the load torque is given to the IM drive. The speed and R_s is estimated very well, which is not affected by the load torque disturbance. The operation of the IM drive is very good and stable during field weakening regions. Thus by using sensor less control IM drive, we can get the same results as that of vector control without using shaft encoder. The complete response at different conditions are obtained and explained in this chapter.

CHAPTER 7

CONCLUSION AND FUTURE SCOPE

7.1 INTRODUCTION

The main focus of the thesis on the estimation techniques for speed and stator resistance sensorless vector control IM drives. The main objective was to estimate the stator resistance and to improve the performance of sensor-less drives which are based on MRAS observers. The focus was given to the critical low speed and zero speed regions of operation. Various MRAS based schemes have been developed and tested as suitable means of producing a satisfactory performance at and around zero speed. The aim of this chapter is to summaries the investigations and findings of this research, present conclusions and recommend various possibilities for future studies.

7.2 MAIN CONCLUSIONS

The presence of a speed sensor in an IM drive may affect the reliability and the cost of the drive system. Therefore the sensor-less control methods offer great advantages. Particular attention was given to MRAS speed observers due to their simple structure and low computational effort.

A state space representation of the IM in the stator reference frame, with the stator currents and the rotor flux linkages components as state variables, has been developed based on the *d*-*q* axes theory. Principles of vector control were also illustrated based on the motor model expressed in the synchronous reference frame. The machine dynamic equations have been used to formulate the MRAS for speed and stator resistance estimation. This scheme is the most common MRAS strategy extensively employed for sensorless control. X-MRAS based model for the estimation of stator resistance is developed and presented in this thesis. The developed algorithm for estimation of R_s is independent of the rotor speed and the estimated R_s is used for the computation of rotor speed, which is observed to be closely tracking the actual speed and is found to be stable for all the four quadrants, even at low speed and zero speed response. Simulations results are used to explain the steady state operation and high dynamic performance of the drive system. The main conclusions that can be drawn from the results are summarized as follow:

- The speed and stator resistance estimator is capable of tracking the stator resistance variations very well. Then the proposed drive scheme can be operated in very low speed range.
- The transient performance of the proposed sensorless drive is presented, when the load torque is given to the IM drive. The speed and R_s is estimated very well, which is not affected by the load torque disturbance.

Thus by using sensor less control IM drive, we can get the same results as that of vector control without using shaft encoder. Hence by using this technique, we can reduce the cost of drive and we can also increase the ruggedness of the drive as well as and its dynamic performance. The usefulness of the proposed algorithm has been confirmed by MATLAB/SIMULINK based simulation.

7.3 FUTURE SCOPE

The work developed in this thesis is based on MRAS techniques which applied to speed sensorless IM vector control drives. Different adaptation mechanisms have been proposed to replace the classical PI controller. The tuning of different parameters has been carried out online by trial and error. A systematic method could be considered for parameter tuning such as use of a GA. Moreover, other optimization algorithms may be considered for minimizing the speed tuning signal.

APPENDIX-A

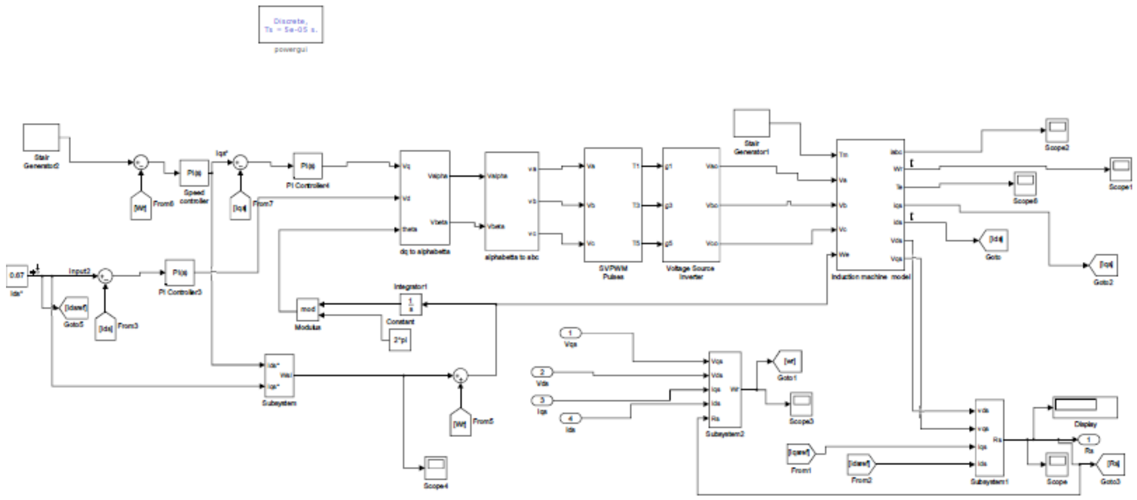

Figure A.1 Simulation Model of IM Drive

REFERENCES

[1] B. K.Bose. 1997. Power Electronics and Variable Frequency Drives. IEEE Press, New York.

[2] Kazmierkowski, R.Krishnan, Blaabjerg, Control in Power Electronics, Selected Problems.

[3] Takahashi Isao, Noguc hi Tos hihiko, „"A New Quick-Response and High-Efficiency Control Strategy of an Induction Motor"", *IEEE Transactions on Industry Applications*, Vol. IA-22 No-5, Sept/Oct 1986.

[4] J. W. Finch and D. Giaouris, "Controlled AC Electrical Drives," *IEEE Transactions on Industrial Electronics*, vol. 55, no. 1, pp. 1-11, February 2008.

[5] P. Vas, *Sensorless Vector and Direct torque control.* New York: Oxford University Press, 1998.

[6] J. Holtz, "Sensorless control of induction motor drives," *Proc. of the IEEE,* vol.90, no. 8, pp. 1359-1394, August 2002.

[7] J. Holtz and J. Quan, "Drift and parameter compensated flux estimator for persistent zero stator frequency operation of sensorless controlled induction motors," IEEE Transactions on Industry Applications, vol. 39, no. 4, pp. 1052- 1 060, July/August 2003.

[8] M. Rashed and A. F. Stronach, "A stable back-EMF MRAS-based sensorless low speed induction motor drive insensitive to stator resistance variation," lEE Proceedings Electric Power Applications, vol. 151, no. 6, pp. 685-693, November 2004.

[9] G. Kohlrusz, D. Fodor, "Comparison of Scalar and Vector Control strategies of Induction motor", Hungarian Journal of Industrial Chemistry, 2011, Vol. 39 (2), pp no. 265-270.

[10] Mohan, Ned. Advanced Electric Drives Analysis Control and Modelling. Minneapolis : MNPERE, 2001.

[11] HOLTZ, JOACHIM. Sensorless Control of Induction Motor Drives. Wuppertal : IEEE, VOL. 90, NO. 8, 2002.

[12] Earl C. Barnes, “Performance and Characteristics of Induction Motors for Solid-State Variable Frequency Drives,” IEEE Transactions on Industry and General Applications Year: 1971, Volume: IGA-7, Issue: 2 Pages: 212 – 217.

[13] Trevor L. Grant and Thomas H. Barton, “Control Strategies for PWM Drives” IEEE Transactions on Industry Applications Year: 1980, Volume: IA-16, Issue:2 Pages: 211 – 216**.**

[14] Bikram Das and Medaaibok Fancon, “Comparison of different PWM-VSI fed 3 Φ IM based on modulation index and switching frequency,” Electrical, Electronics, Signals, Communication and Optimization (EESCO), 2015 International Conference on Year: 2015, Pages: 1 – 6.

[15] Marlen Varnovitsky, “Development and Comparative Analysis of a Pulse-Width Modulation Strategy,” IEEE Transactions on Industrial Electronics, Year: 1984, Volume: IE-31, Issue: 3, Pages: 272 – 276.

[16] Jie Zhang and V. Thiagarajan, “New approach to field orientation control of a CSI induction motor drive,” IEE Proceedings B - Electric Power Applications, Year: 1988, Vol.135, Issue:1, Pages: 1 – 7.

[17] Jie Zhang, “High performance control of a three-level IGBT inverter fed AC drive”,Industry Applications Conference, 1995. Thirtieth IAS Annual Meeting, IAS '95., Conference Record of the 1995 IEEE Year: 1995, Volume: 1 Pages: 22 – 28.

[18] Adel Aktaibi *& Daw Ghanim.* "Dynamic Simulation of a Three-Phase Induction Motor Using Matlab Simulink", Newfoundland Electrical and Computer Eng. Conference (NECEC 2011).

[19] LEONHARD, W. "Control of electrical drives' (Springer Verlag", 1985)

[20] VAS, P.: 'Vector control of AC machines' (Clarendon Press, Oxford, 1990)

[21] P.M Menghal, A Jaya Luxmi, "Dynamic Modeling, Simulation & Analysis of Induction Motor Drives" IEEE International Conference on Power, Energy and Control (ICPEC-13), 6-8 Feb 2013, pp 566-571.

[22] Raad S. Fayath, Mostafa M.Ibrahim, Majid A. Alwan & Haroutuon A. Hairik, "Simulation of Indirect Field-Oriented Induction Motor Drive System Using Matlab/Simulink" J.Basrah Researches (Sciences) Vol.31. Part.1. 83-94 (2005) .

[23] S. Wade, M. W. Dunnigan and B. W. Williams, "Modeling and simulation of induction machine vector control with rotor resistance identification", IEEE Transactions on Power Electronics, vol. 12, No. 3, May 1997, pp. 495–506.

[24] S. Wade, M. W. Dunnigan and B. W. Williams, " Parameter identification for vector controlled induction machines",Control, 1994. Control '94. International Conference on Year: 1994, Volume: 2, Pages: 1187 – 1192.

[25] K. L. Shi; T. F. Chan and Y. K. Wong, "Modelling of the three-phase induction motor using SIMULINK", Electric Machines and Drives Conference Record, 1997. IEEE International,Year: 1997, Pages: WB3/6.1 - WB3/6.3.

[26] B. Ozpineci and L. M. Tolbert, "Simulink implementation of induction machine model - a modular approach", Electric Machines and Drives Conference, 2003. IEMDC'03. IEEE International, Year: 2003, Volume: 2, Pages: 728 – 734.

[27] S. Ayasun and C. O. Nwankpa, “Induction motor tests using MATLAB/Simulink and their integration into undergraduate electric machinery courses”, IEEE Transactions on Education, Year: 2005, Volume: 48, Issue: 1,Pages: 37 – 46.

[28] K.S. Graeid, H.W. Ping, and H.A.F. Mohamed, “Simulink Representation of Induction Motor Reference Frames,” in Proceedings of the 2009 International Conference for Technical Postgraduates (TECHPOS), 2009, pp. 1-4.

[29] O. D. Momoh, “Dynamic Simulation of Cage Rotor Induction Machine – A Simplified and Modular Approach,” in *Proceedings of the 44th IEEE Southeastern Symposium on System theory*, 2012, pp.200-203.

[30] L. Umanand and S. Bhat, “Online estimation of stator resistance of an induction motor for speed control applications,” *IEE Proc. Electr. Power Appl.*, vol. 142, pp. 97–103, Mar. 1995.

[31] A. M. El-Sawy, Yehia S. Mohamed and A. A. Zaki, “Stator Resistance and Speed estimation for Induction Motor Drives As Influenced by Saturation” *Online Journal on Electronics and Electrical Engineering (OJEEE) Vol. (3) – No. (2).*

[32] Gregor Edelbaher and Karel Jezernik, “Low-Speed Sensorless Control of Induction Machine,” IEEE Transactions on Industrial Electronics, Vol. 53, No. 1, February 2006, pp. 120-129.

[33] Nik Idris, Ahmad Razami Haron and Nik Rumzi, “Simulation of MRAS- based Speed Sensorless Estimation of IMD Using MATLAB/SIMULINK,” First International Power and Energy Conference PEC, pp. 411-415, Nov. 2006.

[34] B.Mouli Chandra and S.Tara Kalyani, “Online Estimation of Stator Resistance in Vector Control of Induction Motor Drive”, Power India Conference, 2012 IEEE Fifth,pp. 1-5, 2012

[35] C. Chakraborty, A.V. Ravi Teja, S.Maiti, Y. Hori; "A VxI based adaptive speed sensorless four quadrant vector controlled induction motor drive"; *International Power Electronics Conference (IPEC) 2010*; pp. 3041-3048; June 2010

[36] V.Vasic, S.N.Vukosavic, and Emil Levi; "A Stator Resistance Estimation Scheme for Speed Sensorless Rotor Flux Oriented Induction Motor Drives"; *IEEE Transactions On Energy Conversion*, Vol. 18, No. 4, pp. 476-483, December 2003.

[37] A. V. Ravi Teja, C. Chakraborty, S. Maiti, and Y. Hori; "A New Model Reference Adaptive Controller for Four Quadrant Vector Controlled Induction Motor Drives"; *IEEE Transactions on Industrial Electronics*, Vol. 59, No. 10, pp. 3757-3767, October 2012.

[38] Aswathy Vijay and Binojkumar, "Speed and Stator Resistance Estimation of four quadrant vector controlled IM drives", Int. Journal of Adavanced Research In Electrical, Electronics And Instrumentation Engineering, vol.3, no.5, pp. 329-337, Dec.2014.

[39] C. Schauder, "Adaptive speed identification for vector control of induction motor without rotational transducers," in Conf. Rec. IEEE-IAS. Annual Meeting, 1989, pp. 493–499.

[40] G.Yang and T.H. Chin, "Adaptive speed identification scheme for vector controlled speed sensor-less inverter-induction motor drive", Industry Applications Society Annual Meeting, Conference Record of the 1991 IEEE, Pages: 404 – 408, vol.1.

[41] Young-Real Kim, Seung-Ki Sul and Min-Ho Park, "Speed sensorless vector control of induction motor using extended Kalman filter", IEEE Transactions on Industry Applications Year: 1994, Volume: 30, Issue: 5, Pages: 1225 – 1233.

[42] Min-Huei Kim and J. C. Hung, "Vector control system for induction motor without speed sensor at very low speed", Industrial Electronics, Control, and

Instrumentation, 1995., IEEE IECON 21st International Conference on Year: 1995, Vol.1, pp no. 524-529.

[43] S. Wade; W. Dunnigan and B. W. Williams, “A new method of rotor resistance estimation for vector-controlled induction machines”, IEEE Transactions on Industrial Electronics, Year: 1997, Volume: 44, Issue: 2, Pages: 247 – 257.

[44] Gregor Edelbaher, Karel Jezernik, and Evgen Urlep, "Low-speed sensorless control of Induction machines." IEEE Trans. On Ind. Electr., Vol, 53, No.1, February 2006, PP. 120-129.

[45] P. C. KRAUSE,” Simulation of Symmetrical Induction Machinery”, IEEE Transactions on Power Apparatus and Systems, vol. pas-84, no. 11,pp 1038-1053, November 1965

[46] S. Maiti, V. Verma, C. Chakraborty, and Y. Hori, “An adaptive speed sensorless induction motor drive with artificial neural network for stability enhancement,” *IEEE Trans. Industrial Informatics*, vol. 8, no. 4, pp.757–766, Nov. 2012.

[47] S. Maiti, C. Chakraborty, Y. Hori, and M. C. Ta, “Model reference adaptive controller-based rotor resistance and speed estimation techniques for vector controlled induction motor drive utilizing reactive power,” *IEEE Trans. Ind. Electron*., vol. 55, no. 2, pp. 594-601, Feb. 2008.

[48] M. Rashed and A. F. Stronach, “A stable back-emf mras-based sensorless low speed induction motor drive insensitive to stator resistance variation,” *IEE Proc. of Electric Pow. Applicat.*, vol. 151, no. 6, pp. 685-693, 2004.

[49] R.J.Kerkman, B.J.Seibel,T.M.Rowan, and D.Schlegel,“A new flux and stator resistance identifier for ac drive systems,” *IEEE Trans. Ind. Applicat.*, vol. 32, pp. 585–593, May/June 1996.

[50] T. G. Habetler, F. Profumo, G. Griva, M. Pastorelli, and A. Bettini, “Stator resistance tuning in a stator-flux field-oriented drive using an instantaneous hybrid flux estimator”, *IEEE Trans. Power Electron.*, vol.13, pp. 125–133, Jan. 1998.

[51] I. J. Ha and S. H. Lee, “An online identification method for both stator and rotor resistance of induction motors without rotational transducers,” *IEEE Trans. Ind. Electron.*, vol. 47, pp. 842–853, Aug. 2000.

[52] M. Cirrincione, M. Pucci, G. Cirrincione and G. A. Capolino, “A new adaptive integration methodology for estimating flux in induction machine drives,” *IEEE Trans. Power Electron.*,vol.19,no.1,pp.25–34,Jan.2004.

[53] M. Cirrincione, M. Pucci, G. Cirrincione and G. A. Capolino,“Sensor-less control of induction machines by a new neural algorithm,” *IEEE Trans. Ind. Electron*., vol.54, no.1,pp.127–149, Feb 2007.

[54] M. Tsuji, S. Chen, K. Izumi, and E. Yamada, “A sensor-less vector control system for induction motors using q-axis flux with stator resistance identification,” *IEEE Trans. Ind. Electron*., vol. 48, pp. 185–194, Feb. 2001.

[55] K. Akatsu and A. Kawamura, “Sensorless very low-speed and zero speed estimations with online rotor resistance estimation of induction motor without signal injection,” *IEEE Trans. Ind. Applicat*., vol.36, pp.764–771, May/June 2000.

[56] R. Marino, S. Peresada, and P. Tomei, “On-line stator and rotor resistance estimation for induction motors,” *IEEE Trans. Contr. Syst. Technol*., vol. 8, pp. 570–579, May 2000.

[57] Guidiand H.Umida, “A novel stator resistance estimation method for speed-sensorless induction motor drives,” *IEEE Trans. Ind. Applicat*., vol. 36, pp. 1619–1627, Nov./Dec. 2000.

[58] S. Maitiand and C. Chakraborty, “A new instantaneous reactive power based MRAS for sensor less induction motor drive,” *Simul. Modell. Pract. Theory*, vol.18, no.9, pp.1314–1326, Oct.2010.

[59] F.J.Pengand, T.Fukao, “Robust speed identification for speed sensor less vector control of induction motors,” *IEEE Trans Ind. Appl*., vol.30, no.5, pp.1234–1240, Sep./Oct.1994.

[60] S. Maiti, C. Chakraborty, Y.Hori, and M.C. Ta, “Model reference adaptive controller-based rotor resistance and speed estimation techniques for vector controlled

induction motor drive utilizing reactive power," *IEEE Trans. Ind. Electron.*, vol.55, no.2, pp.594–601, Feb.2008.

[61] Ashutosh Mishra and Prashant Choudhary, "Speed Control of An IM by Using Indirect Vector Control Method," Int. Journal of Emerging Technology and Advanced Engineering, vol.2, Issue 12, pp. 144-150, Dec.2012.

[62] G. Pydiraju and M. Daivaasirvadam, "Sensorless Speed Control of Induction Motor Using MRAS," Int. Journal of Recent Technology and Engineering (IJRTE), vol.1, Issue 5, pp. 31-35, Nov.2012.

[63] Mugdha Bhandari, Shivaji Gavade and Shwetha S H, " Model Reference Adaptive Technique for Sensorless Speed Control of IM Using MATLAB/SIMULINK," Int. Journal of Emerging Technology in Computer Science and Electronics (IJETCSE), vol.14, Issue 2, pp. 112-115, April 2015.

[64] G. Victor Raj, K. Venkataramana and V. Chaitanya, " Predictive Vector Control Based IMD Using Fuzzy Controller," Int. Journal of Science Engineering and Technology Research, vol.4, Issue 11, pp. 4018-4025, Nov.2015.

[65] Dr. Ch. Chengaiah and I Siva Prasad (M. Tech), "Performance of Induction Motor Drive by Indirect Vector Controlled Method Using PI and Fuzzy Controllers", International Journal of Science, Environment and Technology, Vol. 2, No 3, pp. 457 – 469, May 2013.

[66] Zhifeng Zhang, Renyuan Tang, "Novel Direct Torque Control Based on Space Vector With Modulation Adaptive Stator Flux Observer for Induction Motors" *IEEE Transactions on Magnetics*, Vol. 46, No. 8, August 2010.

LIST OF PUBLICATIONS

1. Avinash and M. sreejeth , "Estimation of Stator Resistance in Sensor-less Induction Motor Drive using MRAS", accepted in IEEE Conf. ICPEICES-2016.